Molecular Biology of the Cell
Vol. 16, 5316–5333, November 2005

Microarray Analyses of Gene Expression during Chondrocyte Differentiation Identifies Novel Regulators of Hypertrophy

Claudine G. James,*† C. Thomas G. Appleton,*† Veronica Ulici,*† T. Michael Underhill,*‡ and Frank Beier*†§

*CIHR Group in Skeletal Development and Remodeling and †Department of Physiology and Pharmacology, University of Western Ontario, London, Ontario N6A 5C1, Canada; ‡Department of Anatomy, Cell Biology and Physiology, University of British Columbia, Vancouver, British Columbia V6T 1Z3, Canada; and §School of Dentistry, University of Western Ontario, London, Ontario N6A 5C1, Canada

Submitted February 1, 2005; Revised June 24, 2005; Accepted August 24, 2005
Monitoring Editor: Marianne Bronner-Fraser

Ordered chondrocyte differentiation and maturation is required for normal skeletal development, but the intracellular pathways regulating this process remain largely unclear. We used Affymetrix microarrays to examine temporal gene expression patterns during chondrogenic differentiation in a mouse micromass culture system. Robust normalization of the data identified 3300 differentially expressed probe sets, which corresponds to 1772, 481, and 249 probe sets exhibiting minimum 2-, 5-, and 10-fold changes over the time period, respectively. GeneOntology annotations for molecular function show changes in the expression of molecules involved in transcriptional regulation and signal transduction among others. The expression of identified markers was confirmed by RT-PCR, and cluster analysis revealed groups of coexpressed transcripts. One gene that was up-regulated at later stages of chondrocyte differentiation was Rgs2. Overexpression of Rgs2 in the chondrogenic cell line ATDC5 resulted in accelerated hypertrophic differentiation, thus providing functional validation of microarray data. Collectively, these analyses provide novel information on the temporal expression of molecules regulating endochondral bone development.

INTRODUCTION

Two processes, intramembranous ossification and endochondral ossification, govern the development of the vertebrate skeleton. Bone derived from the former process develops directly from mesenchymal progenitor cells, whereas the latter forms by way of a cartilage intermediary (Cancedda *et al.,* 2000; Karsenty and Wagner, 2002; Eames *et al.,* 2003). Endochondral bone formation proceeds through the formation of a cartilage intermediate that can be further subdivided into two phases: chondrogenesis and chondrocyte differentiation. The commitment of undifferentiated mesenchymal precursor cells to the chondrogenic lineage signals the onset of this process where chondroprogenitors form cellular condensations and differentiate into chondroblasts (Hall and Miyake, 1992; Shum and Nuckolls, 2002). In the second phase, subsets of newly formed chondrocytes become mitotically active, proliferate for an interlude, exit the cell cycle, hypertrophy, and terminally differentiate. End stage chondrocytes undergo apoptosis and are replaced by bone cell precursors (Akiyama *et al.,* 2002; Kronenberg, 2003). These later phases of chondrocyte proliferation and differentiation occur in the growth plate at the cartilage-bone interface. This region therefore controls longitudinal growth of endochondral bones through the multiplication and hypertrophy of chondrocytes.

Complex regulatory and signaling networks involving cell-matrix and intercellular interactions, coupled to tightly regulated gene expression, mediate the successive stages of proliferation and differentiation that produce all cellular states observed in the growth plate (DeLise *et al.,* 2000). Proteins of numerous molecular families have been implicated in the longitudinal growth of the skeleton including growth factors, e.g., bone morphogenetic proteins, fibroblast growth factor family members, insulin-like growth factor signaling components (Cancedda *et al.,* 1995); extracellular matrix molecules, e.g., collagen II, aggrecan, link protein and cartilage oligomeric protein (Cheah *et al.,* 1991; Watanabe *et al.,* 1994; Fang *et al.,* 2000; Tuckermann *et al.,* 2000); and transcription factors, e.g., Sox9, Core-binding factor alpha (Cbfa1) and ATF-2. In particular, Sox9 has been shown to be required for chondrogenesis, ATF-2 controls cell cycle progression and proliferation, and Cbfa1/Runx2 is involved in hypertrophic differentiation (Reimold *et al.,* 1996; Lefebvre and de Crombrugghe, 1998; Beier *et al.,* 1999; Bi *et al.,* 1999; Stricker *et al.,* 2002).

The intricate nature of cartilage development makes strict coordination between the various chondrogenic factors imperative for the establishment and maintenance of normal growth plate physiology. Improper regulation of genes belonging to the associated functional categories has been linked to growth disturbances and pathological conditions (Ballock and O'Keefe, 2003). For example, achondrodysplasias, hypochondrodysplasias, and thanatophoric dysplasia have been associated with activating mutations in the *Fgfr3*

This article was published online ahead of print in *MBC in Press* (http://www.molbiolcell.org/cgi/doi/10.1091/mbc.E05–01–0084) on August 31, 2005.

Address correspondence to: Frank Beier (fbeier@uwo.ca).

gene, encoding fibroblast growth factor receptor 3, an important modulator of growth plate function (Ornitz, 2001). In addition, the pathogenesis of osteoarthritis is thought to reiterate changes occurring during normal cartilage development (Gelse *et al.*, 2003).

Although many of the molecular players involved in chondrogenic differentiation have been identified, a comprehensive understanding of the mechanisms governing endochondral bone formation has not been achieved. Our knowledge of essential intracellular signaling cascades is especially limited. The advent of functional genomics in combination with systems biology and integrative physiology approaches has equipped us with the tools to overcome some of the challenges associated with understanding complex developmental processes.

In this study, comprehensive gene expression profiling of the in vitro murine micromass culture system has been used to systematically investigate temporal modulation of factors that coordinate chondrogenesis and chondrocyte differentiation. These studies identified numerous genes that undergo significant changes in expression during chondrogenic differentiation. One of these genes, the regulator of G-protein signaling 2 (*Rgs2*) gene was selected for functional analyses that demonstrated novel functional roles of Rgs2 in hypertrophic chondrocyte differentiation. The data presented here will further our understanding of normal endochondral bone formation and consequently the impact of pathological perturbations on the developing skeleton.

MATERIALS AND METHODS

Murine Micromass Cultures and RNA Isolations

Micromass cultures were prepared as described (Ahrens *et al.*, 1977; Cash *et al.*, 1997; Weston *et al.*, 2000; Stanton *et al.*, 2004) with minor modifications. Forelimbs and hindlimbs from 8 to 12 litters of E11.5 CD1 mouse embryos (obtained from Charles River Laboratories, Montreal, Quebec, Canada) were removed and segmented in Puck's Saline A buffer (PSA). The isolated limb buds were dissociated in 10 mg/ml dispase (Roche Molecular Biochemicals, Indianapolis, IN) solution containing 10% fetal bovine serum (FBS)/PSA for 1.5 h at 37°C and shaken at 100 rpm. The enzymatic reaction was neutralized with 2:3 DMEM (Wisent, St.-Bruno, Quebec, Canada): F12 media containing 10% FBS (Invitrogen, Life Technologies, Burlington, Ontario, Canada). Digested limbs were subsequently passed through a 40-μm cell strainer (Falcon, Lincoln Park, NJ) to obtain a single cell suspension and were briefly centrifuged. Cells were resuspended in growth media at a concentration of 2.5×10^7 cell/ml and spotted in 10 10-μl droplets per well of a six-well NUNC cell culture plate. After cells adhered to culture dishes for 1 h at 37°C in a humidified atmosphere containing 5% CO_2, 2 ml of 2:3 DMEM/F12 media containing 10% FBS, 0.5 mM glutamine, 25 U penicillin/ml, and 25 μg streptomycin/ml was added. The medium was supplemented with 0.25 mM ascorbic acid (Sigma, Oakville, Ontario, Canada) and 1 mM β-glycerophosphate (Sigma) to differentiate cultures (Stanton *et al.*, 2004). Growth media were replaced daily, and total RNA was extracted on days 3, 6 9, 12, and 15 of culture with the Qiagen RNA easy kit according to the manufacturer's instructions (Chatsworth, CA). RNA quantity and quality was subsequently confirmed with Agilent 2100 BioAnalyzer Data Review Software (Wilmington, DE) at the London Regional Genomics Center.

Staining Methods

Cells were stained for chondrogenic differentiation with Alcian blue, which binds sulfated proteoglycans. Cells were washed twice with phosphate-buffered saline (PBS) and fixed for 2 h in a 10% Formalin solution. Alcian blue was added to cells and allowed to incubate at room temperature for 2 h. Excess stain was removed and cells were rinsed twice with 70% ethanol to remove residues before visualization (Stanton *et al.*, 2004).

Alkaline phosphatase (ALP) activity was visualized as described (Stanton *et al.*, 2004). For micromass staining, cells were washed twice in cold PBS, and micromass cultures fixed with 10% Formalin for 2 h at room temperature. ATDC5 cells were fixed in cold 95% ethanol for 20 min at −20°C. Cells were subsequently rinsed twice and incubated in water (pH 8.0) for 15 min. A solution containing 0.1 mg/ml naphthol AS-MX phosphate (Sigma), 0.5% *N,N*-dimethylformamide, 2 mM $MgCl_2$, and 0.6 mg/ml Red Violet LB salt (Sigma) in 0.1 M Tris/HCl (pH 8.3) was added to the cells, and the cultures were placed in dark conditions for 45 min. Cells were air-dried before computer scanning and visualization.

Von Kossa staining was utilized to visualize calcium deposition in micromass cultures. Cells were washed twice with cold PBS and fixed with 10% Formalin for 2 h at room temperature. Cells were stained first for ALP before staining with 2.5% (wt/vol) silver nitrate solution for 30 min to increase contrast. After washing with water, cells were air-dried before visualization (Stanton *et al.*, 2004).

Microarray Analysis

Expression analysis of known chondrogenic markers *Sox9* and *Ibsp* (Bone sialoprotein [BSP]) using real-time PCR in three independent micromass trials was completed as described (Stanton *et al.*, 2004) before microarray analysis to validate RNA quality and to verify chondrogenic differentiation in these trials. Total RNA from the three biological replicates were subsequently analyzed with the Agilent Bioanalyzer 2100 system at the London Genomics Facility to confirm RNA integrity. Hybridization proceeded according to the standard Affymetrix protocol (http://www.affymetrix.com/support/technical/manuals.affx). The MOE430A chip contains oligonucleotides for 22 690 probe sets representing ~14,000 mouse genes.

Data Analysis

Microarray Suite 5.0 and GeneSpring 6.1. The gene expression data were analyzed using the Microarray Suite (MAS) 5.0 algorithm (Affymetrix, Santa Clara, CA) in which all probe sets were scaled to the target value of 150. Pivot files generated through M.A.S. analysis were imported into GeneSpring 6.1 software (Silicon Genetics, Redwood City, CA) for data mining. Data transformation values were set to <0–0.1, and per chip normalizations were set to the 50th percentile in addition to per gene normalizations to the median and to specific samples. Day 3 data from all experimental replicates were defined as the baseline array. Signal intensity values for all experimental replicates on any given time point were averaged and used for additional analysis. The starting data set represented 22,690 probe sets. Additional filtering was executed to reduce type I errors (i.e., false positives), which result from experimental procedures and probe design. Genes assigned an "Absent" call for all time points were eliminated from the data set and 16,709 probe sets remained. M.A.S. 5.0 derived algorithms assign statistically spurious expression values an "Absent" call, which signifies of a decreased likelihood that the corresponding signal intensity obtained from the analysis is a reflection of an actual expressed transcript. This data set was additionally filtered with a one-way Welch ANOVA (p-value cutoff of 0.05) and Benjamini and Hochberg False Discovery Rate testing in order to further reduce the working data set to 3334 probe sets. Probe set lists were filtered using the "Filter on Fold Change" option in GeneSpring. A minimum twofold change in gene expression defined differential expression for this data set.

GeneTraffic. Raw microarray data were also imported into GeneTraffic UNO 3.0 (Iobion Informatics, Stratagene, La Jolla, CA) and normalized according to the Robust Multi-array Analysis summary measure (Irizarry *et al.*, 2003) in which day 3 represented the baseline culture time point. Resulting signal intensities were utilized for subsequent analysis. The 22,690 probe sets were filtered to remove all genes that were not assigned a present call in at least one culture time point. The resulting data set contained 16,256 probe sets. Gene expression values were subsequently filtered in a parallel manner to the list generated in GeneSpring after statistical analysis. Individual probe sets were selected for visualization.

Clustering. Self Organizing Maps (SOMs) were generated using the 3334 probe sets obtained from data analysis in GeneSpring 6.1. The following parameters were used: 7 rows, 6 columns, 220,000 iterations, and a neighborhood radius of 6.0. Genes without data in half of the starting conditions were not used for the analysis. K-means clustering where K = 5 of 3 of the 42 cluster sets created by SOM analysis was executed to generate groups of highly similar probe sets. Standard correlation similarity measures were used along with 10,000 iterations that converged after six iterations to create final cluster sets.

Gene Ontologies. Probe set lists resulting from the comparison of genes expressed on day 3 versus 15 of culture filtered using a twofold cutoff were assigned a molecular function with the fatiGO program (Al-Shahrour *et al.*, 2004; http://fatigo.bioinfo.cnio.es/), using the level two filtering parameter. Probe sets annotated by the Gene Ontology Consortium were selected for analysis. Genes assigned to individual categories listed were calculated based on the proportion of annotated probe sets included in all lists.

RT-PCR

cDNA from the micromass time course was generated with the First-Strand cDNA Synthesis system for RT-PCR using SuperScript II RNase H-Reverse Transcriptase (Invitrogen Life Technologies), random hexamers (Invitrogen Life Technologies) and p(dT) 12–18 (Invitrogen Life Technologies). RT prod-

ucts were generated according to the manufacturer's specifications using 1 μg of RNA and a 50-min incubation period at 42°C. A 15-min cDNA incubation at 65°C terminated the reaction. PCR was executed in 50-μl reaction volumes containing 1 μl RT products and 0.5 μl of AmpliTaq Gold polymerase (Perkin Elmer-Cetus, Boston, MA). Amplification conditions for primers began with a 1.5-min denaturation step at 95°C, with annealing temperatures ranging from 50 to 63°C with a 72°C extension phase. PCR reactions occurred over 25–32 cycles, and the reaction was terminated with a 6-min final extension phase at 72°C. PCR products were visualized with UV light after electrophoresis of a 1% agarose gel containing ethidium bromide. For primer sequences, see Table 3.

In Situ Hybridization

PCR products from RT-PCR amplification of murine *Rgs2* mRNA (see Table 3 for primer sequences) were cloned into pGEM T-Easy vector (Promega, Madison, WI), and clones were validated by sequencing. Linearized pGEM-Rgs2 vector was used to generate sense (via T7 RNA Polymerase) and antisense (via SP6 RNA Polymerase) DIG-labeled riboprobes using 10X DIG Labeling Mix (Roche).

Limbs from embryonic day 15.5 mice (E15.5) were fixed overnight with 4% paraformaldehyde (PFA) in PBS, pH 7.4, at 4°C, washed overnight with PBS (4°C), dehydrated, and embedded in paraffin. Sections of 10 μm were cut, mounted on 3-aminopropyltriethoxy-silane-treated (positively charged) glass slides, dewaxed in xylenes, and rehydrated. After washing in PBS, they were digested with 10 μg/ml proteinase K, fixed in 4% PFA, and acetylated with 0.25% acetic anhydride. The sections were hybridized overnight at 55°C with DIG-labeled riboprobes for *Rgs2* (sense or antisense). After hybridization, the sections were washed in 2× SSC, 1× SSC, and 0.5× SSC at 50°C. Riboprobes were digested with RNase A and washed once with tris-buffered saline (TBS; pH 7.5). Anti-DIG antibody conjugated to ALP (Roche) was used as the primary antibody. The blocking and detection of the DIG-labeled sections using NBT-BCIP colorimetric reaction was carried out according to the instructions of the manufacturer (Roche).

Generation of Stable Transfectants and ATDC-5 Cell Culture

ATDC5 cells were cultured and transfected as described (Wang *et al.*, 2004). For transfections, cells were seeded at 2×10^4 cells/ml per well of six-well tissue culture plates and individually transfected with expression vectors for human RGS2 (Guthrie cDNA Resource Center, http://www.cdna.org/) and empty expression vector pcDNA3.1+ (Invitrogen) using Fugene6 (Roche) according to the manufacturer's specifications. Pools of transfected cells were selected with 800 mg/ml Geneticin. Differentiation was induced by addition of ITS as described (Wang *et al.*, 2004).

Western Blotting

ATDC5 cells were centrifuged at $1000 \times g$ in ice-cold PBS and resuspended in ice-cold RIPA lysis buffer (150 mM NaCl, 50 mM Tris-HCl, pH 7.5, 1% Triton X-100, 1% deoxycholate, 0.1% SDS, 2 mM EDTA, 500 mM sodium fluoride, 100 mM sodium orthovanadate). Cell lysates were subsequently sonicated and the protein was quantified by bicinchoninic acid (BCA) assay (Sigma) according to the manufacturer's specifications. To confirm expression of HA-tagged RGS2, 60 μg of protein was loaded and size-fractionated on a 10% SDS-PAGE and blotted overnight onto a nitrocellulose membrane (PROTRAN, Schleicher and Schuell Bioscience, Keene, NH). Nonspecific sites were blocked in a 5% solution of nonfat milk powder in TBS. The nitrocellulose membrane was incubated with high-affinity rat monoclonal anti-HA IgG (Roche) followed by incubation with goat anti-rat secondary IgG antibody with horseradish peroxidase conjugate (Santa Cruz Biotechnology, Santa Cruz, CA) using 1:1000 and 1:5000 dilutions, respectively. Lysates containing HA-tagged constructs were visualized with enhanced chemiluminescence Advance Western blot detection system (Amersham Biosciences, Piscataway, NJ) and Alphaimager 2200.

ALP Activity Assay

Enzymatic activity was measured as described (Stanton *et al.*, 2004) by washing the cells with cold PBS, immediately harvesting the cells in a solution of 10 mM Tris-HCl (pH 8.3) containing 0.2% IGEPAL, and storing the samples at −20°C until the enzymatic activity was measured. Samples were thawed on ice and sonicated. The ALP substrate, *p*-nitrophenyl phosphate substrate (Sigma), was added to the sample supernatants and kept in dark conditions. Sodium hydroxide (3 M) was added to the reaction to terminate substrate hydrolysis after 15 min. The absorbance at 405 nm was used to quantify the amount of *p*-nitrophenyl substrate liberated by ALP activity. The samples were normalized to their protein concentration (mg/ml) with the bicinchoninic acid assay (Sigma) according to the manufacturer's guidelines.

Real-Time PCR

Real-Time PCR was performed to quantitatively assess RNA samples according to (Stanton *et al.*, 2004). Primer and probe sequences for TaqMan GAPDH control reagents were used as an internal control, because this gene demonstrated less variability and greater reproducibility in our system (compared with other standardization probes such as 18s RNA). The GAPDH primer probe set was 5′-GAAGGTGAAGGTCGGAGTC-3′ for the forward primer; 5′-GAAGATGGTGATGGGATTTC-3′ for the reverse primer and JOE-CAAGCTTCCCGTTCTCAGCC-TAMRA for the probe. Specific target primers and probes for Fgfr3 and Ihh with primers and probes generated from Applied Biosystems TaqMan Assays-on-Demand consisting of two unlabeled primers and FAM (6-carboxyfluorescein) dye-labeled TaqMan MGB probe in addition to primer and probe sets for Sox9, Col2a1, and BSP as described (Stanton *et al.*, 2004). Individual primer pairs along with their corresponding probes and template RNA were combined with TaqMan one-step mastermix kit (Applied Biosystems) up to a total volume of 15 μl. The ABI Prism 7900 HT sequence detector (Perkin Elmer-Cetus) was used to detect the amplified target sequences. The primers were annealed at 60°C for 40 PCR cycles. Experimental values represent reaction mixtures completed in triplicate for each time point, and data are a compilation of a minimum of three experimental trials. Negative controls include the mastermix without template RNA. Real-time expression values were calculated using the relative standard curve method. Standard curves were generated for both the target of interest and the endogenous control (GAPDH) by measuring the cycle number at which exponential amplification occurred in a dilution series of samples with known concentrations (plotted as the log concentration). The level of target and endogenous control transcripts were calculated by solving for the *x*-intercept of the slope of the standard curve line. Normalized target values were subsequently generated by taking the antilog of the *x*-intercept and finally taking the quotient of the amounts of target and endogenous control

RESULTS

Validation of Micromass Culture System

We used micromass cultures as an established in vitro model system for chondrogenesis and chondrocyte differen-

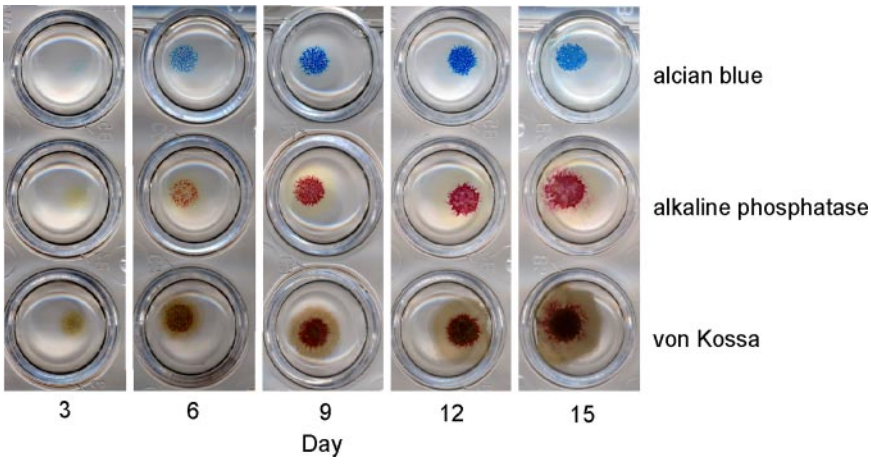

Figure 1. Qualitative characterization of micromass cultures. Images of micromass cultures undergoing chondrogenesis and chondrocyte differentiation on days 3, 6, 9, 12, and 15 of culture are represented. Cells were stained with Alcian blue to show synthesis of sulfated glycosaminoglycans, for ALP activity and with von Kossa for mineralization. All markers increase throughout the culture period.

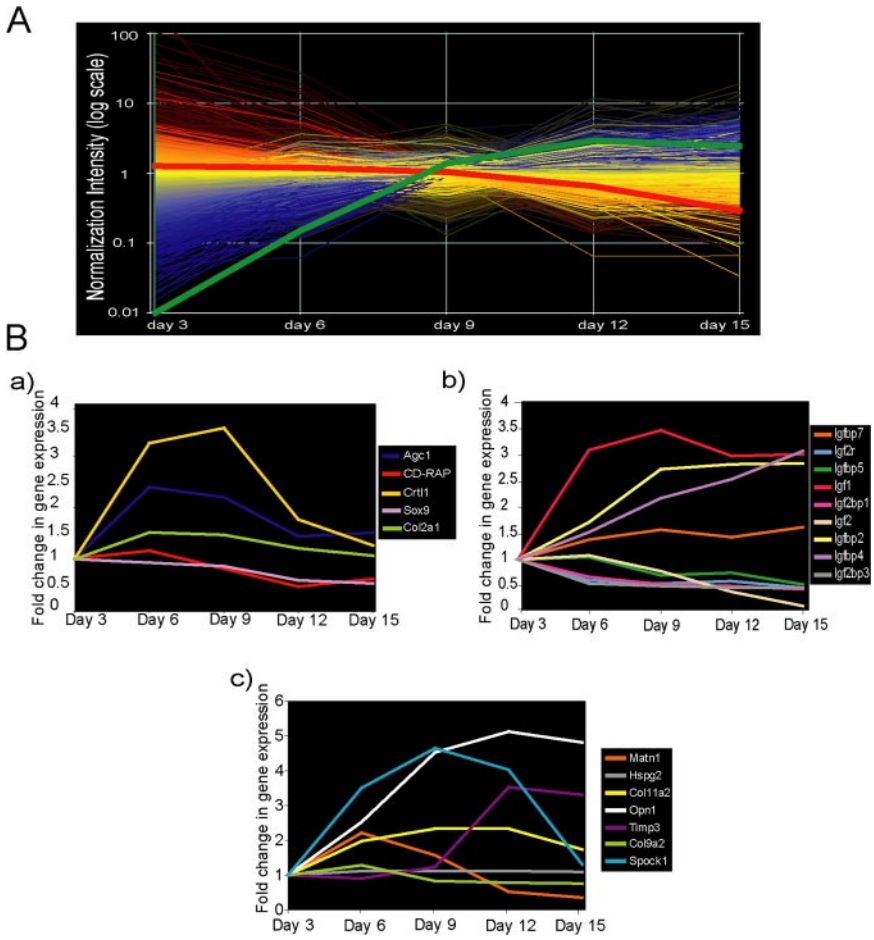

Figure 2. Affymetrix microarray analysis of chondrogenesis and chondrocyte differentiation. Total RNA from the micromass time course was hybridized to Affymetrix MOE430A chips containing ~14,000 murine genes. Data from three biological replicates are shown. Preliminary analysis in M.A.S 5.0 and GeneSpring 6.1, in which all probe sets were subject to various filters (see *Materials and Methods*), resulted in the creation of data set consisting of 3334 probes sets. Expression profiles for *Sox9* and *Ibsp* are highlighted in red and green, respectively (A). Expression patterns for additional characterized cartilage markers such as Aggrecan (*Agc1*), cartilage-derived retinoic acid-sensitive protein (*Cdrap*), Sox9, Link protein (*Crtl1*), and Collagen II (*Col2a1*) are also shown (Ba). Expression patterns of IGF signaling constituents are shown (Bb). Transcripts involved in extracellular matrix signaling including matrilin (*Matn1*), perlecan (*Hspg2*), collagen 11a1 (*Col11a1*), osteopontin (*Opn1*), tissue inhibitor of metalloproteinase 3 (*Timp3*), collagen 9a2 (*Col9a2*), and osteonectin (*Spock1*) are shown (Bc). Genes such as insulinlike growth factor binding protein 6 (*Igfbp6*) and matrix metalloprotease 13 (*Mmp13*), Ibsp, a disintegrin and metalloprotease domain 23 (*Adam23*), and cartilage oligomeric protein (*Comp*) exhibit greater than fivefold changes in gene expression and are not shown for scaling reasons. (B). All values reflect fold changes in gene expression relative to day 3 of micromass culture.

tiation of mouse mesenchymal cells (Cormier *et al.,* 2003; Stanton *et al.,* 2004; Zhang *et al.,* 2004). Cultures were qualitatively assessed with Alcian blue, ALP and von Kossa staining on days 3, 6, 9,12, and 15 of the time course. In all cases, staining intensity increases over time confirming the progression of the cultures along the chondrogenic lineage (Figure 1). Quantitative Real-Time PCR analysis of the micromass cultures revealed that expression of well-characterized markers of chondrocyte differentiation, namely *Sox9* and *Ibsp,* follow expected expression patterns (Chen *et al.,* 1992; Bi *et al.,* 1999; unpublished data). *Sox9* mRNA showed peak expression during days 3 and 6 of the culture period, after which transcript levels decreased by 50% in parallel with the maturation of differentiated chondrocytes. The opposite pattern was observed for *Ibsp* transcripts, which showed very low expression until days 12 and 15 of culture when cartilage cells terminally differentiate and up-regulate *Ibsp* mRNA levels 1200-fold.

Microarray Analyses

Total RNA isolated from the micromass cultures in 3-d increments over a 15-d time course were hybridized to the Affymetrix MOE430A arrays containing 22,690 probe sets representing nearly 14,000 mouse genes (Figure 2A). Analysis in GeneSpring 6.1 software demonstrated that ~3300 transcripts from a total of 16,709 probe sets are expressed in at least one time point during the culture period (for details see Materials and Methods). Expression profiles of *Sox9* and *Ibsp* were consistent with the trends observed by real-time PCR (Figure 2A). Closer inspection of expression trends for additional known chondrogenic markers also followed the expected patterns (Figure 2Bb). Specifically, the expression of the proteoglycans Aggrecan (*Agc1*) and link protein (*Crtl1*; Watanabe *et al.,* 1998) were similar, though link protein exhibited greater fold differences. Microarray analysis demonstrates that *Agc1* and *Crtl1* transcripts increased from the beginning of the culture period toward day 6, remained at similar levels until day 9, and subsequently decreased for the remainder of the time course. Similar patterns, although less pronounced, were found for other cartilage markers such as *Col2a1* and *Cdrap* consistent with their expression in vivo (Dietz and Sandell, 1996). Further examination of molecules implicated in formation and remodeling of the cartilage extracellular matrix such as matrilin 1 (*Matn1*), perlecan (*Hspg2*), collagen 11a1 (*col11a1*), osteopontin (*Opn1*), tissue inhibitor of metalloproteinase 3 (*Timp3*), collagen 9a2 (*col9a2*), and osteonectin (*Spock1*) also demonstrate expected expression patterns (Figure 2Bc; Pacifici *et al.,* 1990; Kim *et al.,* 1999; Knudson and Knudson, 2001; Eyre, 2004).

The insulinlike growth factor (IGF) signaling system is one of the major regulators of endochondral ossification (Schmid, 1995). We analyzed expression of IGF signaling components in our data sets. Most notably, mRNA encoding IGF1 is markedly up-regulated at later stages of differentiation, along with transcripts for IGF-binding protein (IGFBPs) 2, 4, and 6, whereas IGF2 displays the opposite behavior (Figure 2Bb, Table 1). In particular, IGFBP6 is up-regulated ~11-fold on day 15 versus day 3 of culture and

Table 1. Identification of IGF axis components in cartilage differentiation

Gene name	Fold change
Igfbp7	1.6
Igf2r	−2.2[a]
Igf1	1.6
Igfbp5	−1.9
Igfbp4	2.2
Igf1	3.0
Igf2bp	−2.3
Igf2	−9.2
Igfbp2	2.8
Igfbp4	3.1
Igf2bp3	−2.2
Igfbp6	10.9

[a]Negative values indicate down-regulation.

shows a very similar expression pattern to matrix metalloprotease 13 (*Mmp13*), *Ibsp*, Cartilage Oligomeric Protein (*Comp*) and the newly implicated a disintegrin and metalloprotease domain 23 (*Adam23*), which are examples for end-stage cartilage markers that exhibit greater than fivefold upregulation in gene expression in our array (IGFBP6 could not be shown in Figure 2 for scaling reasons).

Validation of Microarray Expression Data

To validate microarray data using independent methods, both new and novel markers were selected for analysis of micromass gene expression by RT-PCR. Gene expression patterns for cartilage link protein 1 (*Crtl1*), nuclear cap binding protein subunit 2 (*Ncbp2*), and myogenic differentiation 1 (*Myod1*) matched the expression patterns obtained by microarray analysis (Figure 3). *Crtl1* increases from day 3 to day 6 of culture, remains at similar levels until day 9, and subsequently decreases until day 15 of the developmental time line (Figure 3A). The expression pattern of *Ncbp2* demonstrates gradual decrease in gene expression until it reaches a plateau at day 12 of the culture period (Figure 3B). Consistent with our previous results (Weston *et al.*, 2003), *Myod1* is strongly expressed on day 3 of the culture period, followed by a marked decrease in gene expression on day 6 and virtual absence of a signal thereafter (Figure 3C). The microarray expression patterns of these genes can therefore be validated through alternative experimental means, which suggests that microarray data correspond to actual gene expression patterns.

Identification of Trends in Gene Expression

The distribution of differentially expressed probe sets was assessed for the duration of the time course. Specifically, the number of differentially expressed transcripts between sequential time points was compared using various fold change cutoffs (Figure 4A). The largest changes in gene

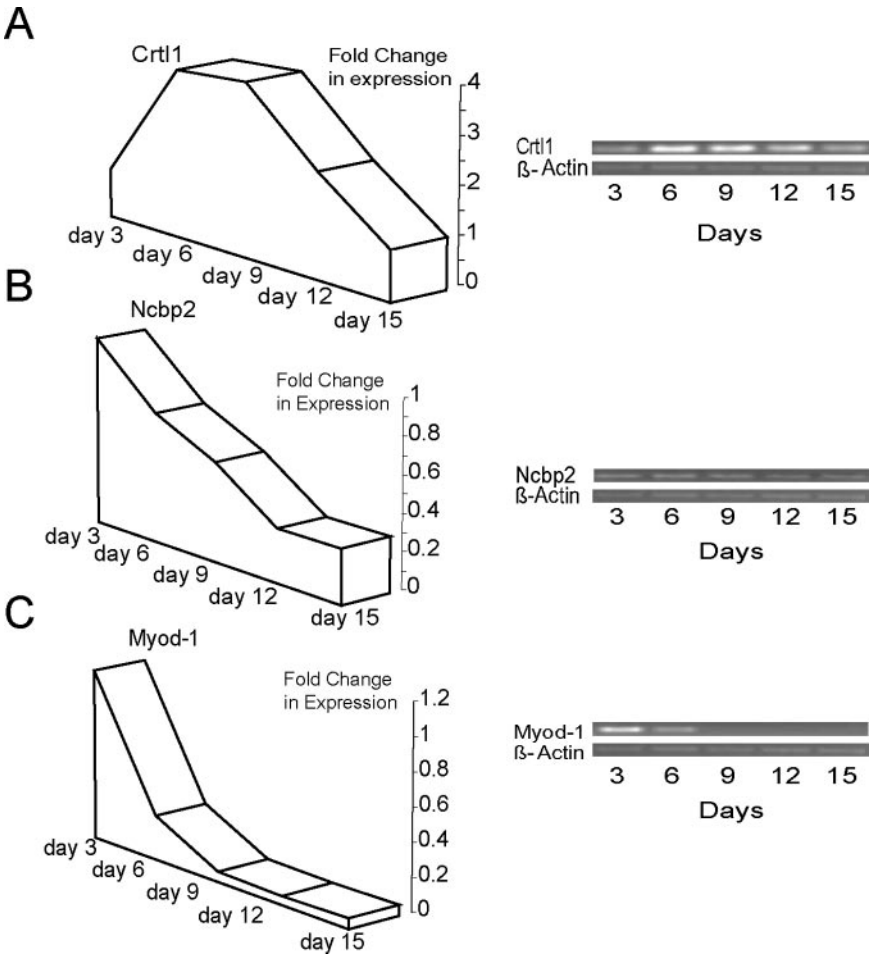

Figure 3. Validation of differentially expressed genes by RT-PCR. Temporal expression patterns of Cartilage Link Protein 1 (*Crtl1*; A), nuclear cap binding protein (*Ncbp2*; B), and myogenesis differentiation factor 1 (*Myod-1*; C) were confirmed by RT-PCR using β-actin as a loading control. The microarray expression profile shown as fold change in expression is shown on the left with the corresponding RT-PCR to the right.

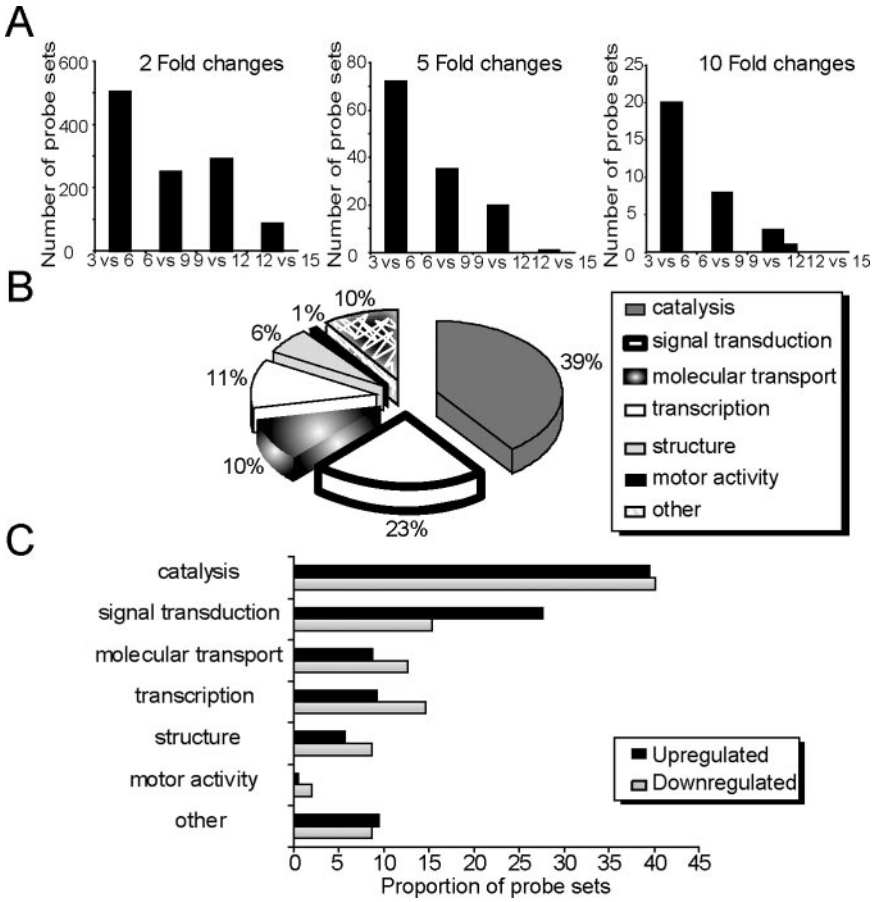

Figure 4. Distribution of differentially expressed probe sets and corresponding molecular classification according to GO terms. Differential gene expression analyzed in succession shows the number of probe sets exhibiting changes as the developmental time line progresses. Probe sets were filtered according to 2-, 5-, and 10-fold change cutoffs (A). Day 3 versus day 6, and day 12 versus day 15 represent the largest and smallest proportion of changes between culture days, respectively. Genes exhibiting minimum twofold changes in gene expression between day 3 and day 15 were assigned molecular function and categorized according to GO annotations assigned in the FatiGO program (B). The proportion of genes that are up- or down-regulated in the gene list derived from twofold changes in gene expression between days 3 and 15 of micromass culture (C).

expression were observed between days 3 and 6 of the time course at all fold change cutoffs. Conversely, the smallest number of genes changed between days 12 and 15 of culture.

Probe set lists for transcripts differentially regulated between day 6, 9, 12, or 15 of culture and the day 3 baseline were examined using 2-, 5-, and 10-fold change cutoffs. Approximately 1772, 481, and 249 probe sets were differentially expressed by 2-, 5-, and 10-fold, respectively, between days 3 and 15 of culture, which coincides with the largest change in gene expression between two nonsequential culture days. Table 2 shows genes demonstrating at least 10-fold changes in expression levels between days 3 and 15. This is consistent with the different stages of cartilage formation: namely chondrogenesis and the terminal differentiation of chondrocytes. Closer examination of these lists involved functional categorization of differentially expressed transcripts in the twofold change category (1772 probe sets). Classification according to GeneOntology (GO) annotations showed that the majority of annotated transcripts were involved in catalysis (39%), signal transduction (23%), and transcriptional regulation (11%). Approximately 10% of transcripts included were not assigned a functional classification (shown as "other"; Figure 4B). Similar distributions were observed for genes with a 5- and 10-fold cutoff (unpublished data).

Differences in the proportion of transcripts showing increased or decreased expression patterns were also assigned to various functional groups. The most pronounced difference occurred in the signal transduction, transcription, and motor activity categories where 1.8-fold more up-regulated transcripts, 1.5-fold more down-regulated transcripts, and 4.4-fold more down-regulated transcripts, respectively, were identified (Figure 4C). These patterns are consistent with gene expression profiles observed for vascular endothelial growth factors and matrix metalloproteases in the case of the signal transduction, *Sox9* and other patterning molecules in the case of transcription, and muscle markers such as myosin in the case of motor activity. The identification of gene expression trends provides insight into the distribution of functional classes that temporally modulate chondrocyte maturation as well as additional support for the micromass culture system as an appropriate in vitro model for chondrocyte differentiation.

Clustering Analyses

Genes exhibiting similar expression pattern may be involved in similar biological processes and may therefore be regulated by similar upstream mechanisms (Marcotte *et al.*, 1999). Thus, we attempted to identify coexpressed genes by cluster analysis. Two clustering methods were used to complete the analysis: SOMs and K-means clustering (see *Materials and Methods* for details). SOMs were executed in GeneSpring using the initial data set consisting of all significantly expressed transcripts. Of the 42 resulting SOMs, three patterns were analyzed in detail. Cluster 1 contained 140 probe sets that are up-regulated toward the end of the developmental program, likely representing transcripts involved in hypertrophic differentiation (Figure 5A, left panel). *Mmp13*, a known marker of late-stage hypertrophic differentiation, is found in this cluster (Tuckermann *et al.*, 2000). Cluster 2 contained 58 transcripts that peak around day 6 and day 9 of

Table 2. Identification of genes differentially expressed between days 3 and 15 of micromass culture

Up-regulated genes

Gene name	Gene description	GO molecular function/GO biological process/ GO cellular component	Fold change
Cxcl16	Chemokine (C-X-C motif) ligand 16	Chemokine activity; cytokine activity; low-density lipoprotein receptor activity; scavenger receptor activity	10
Avil	Advillin	Actin binding	10
Sepp1	Selenoprotein P, plasma, 1	Selenium binding	10
BB327418	Expressed sequence AU043488	Unavailable annotation	11
Fgf21	Fibroblast growth factor 21	Growth factor activity	11
Gpr49	G protein-coupled receptor 49	Protein-coupled receptor activity	11
Igfbp6	Keratin complex 2, basic, gene 8	Growth factor binding; insulinlike growth factor binding	11
Dspg3	Dermatan sulphate proteoglycan 3	Extracellular space	11
Cilp2	Cartilage intermediate layer protein 2	Unavailable annotation	11
BC013672	cDNA sequence BC013672	Unavailable annotation	11
Dcn	Decorin	Extracellular space	11
Tcfec	Transcription factor EC	DNA binding; transcription factor activity	11
Esm1	Endothelial cell-specific molecule 1	Insulinlike growth factor binding	11
Emp2	Epithelial membrane protein 2	Integral to membrane	11
Cpxm2	Carboxypeptidase X 2 (M14 family)	Not carboxypeptidase activity; carboxypeptidase A activity; protein binding	11
Vit	Vitrin	Positive regulation of growth rate	11
Ptpns1	Protein tyrosine phosphatase, non-receptor-type substrate 1	Phosphoprotein amino acid binding; protein binding	11
Serpina3n	Serine (or cysteine) proteinase inhibitor, clade A, member 3N	Endopeptidase inhibitor activity; peptidase activity; serine-type endopeptidase inhibitor activity	11
Krtdap	Keratinocyte differentiation associated protein provided	Unavailable annotation	11
Ctss	Cathepsin S	Cathepsin S activity; cysteine-type endopeptidase activity; cysteine-type peptidase activity; hydrolase activity	12
Cxcl15	Chemokine (C-X-C motif) ligand 15	Chemokine activity; cytokine activity	12
Chrdl1	Chordinlike 1	Development	12
Lmo2	LIM domain only 2	Zinc ion binding	12
Hpgd	Hydroxyprostaglandin dehydrogenase 15 (NAD)	15-hydroxyprostaglandin dehydrogenase (NAD+) activity	12
Fndc1	Fibronectin type III domain containing 1	Unavailable annotation	13
Wisp2	WNT1 inducible signaling pathway protein 2	Calcium ion binding; insulinlike growth factor binding; phospholipase A2 activity; protein binding	13
BC022123	Complement component 1, s subcomponent	Calcium ion binding; chymotrypsin activity; hydrolase activity; peptidase activity; serine-type endopeptidase activity	13
Ccr5	Chemokine (C-C motif) receptor 5	C-C chemokine receptor activity; G-protein-coupled receptor activity; rhodopsin-like receptor activity	13
C1qb	Complement component 1, q subcomponent, beta polypeptide	Complement activation	13
Plek	Pleckstrin	Calcium ion binding	13
Tspan17	Tetraspanin 17	integral to membrane	14
Rassf5	Ras association (RalGDS/AF-6) domain family 5	Protein binding	14
Alox5ap	Arachidonate 5-lipoxygenase activating protein	Enzyme activator activity	14
Adm	Adrenomedullin	Hormone activity; neuropeptide hormone activity	14
AK018128	RIKEN cDNA 6330406I15 gene	Unavailable annotation	14
BC027279	Biliverdin reductase B (flavin reductase (NADPH))	NADPH dehydrogenase activity; biliverdin reductase activity; catalytic activity; oxidoreductase activity	15
Fxyd2	FXYD domain-containing ion transport regulator 2	Ion channel activity; sodium/potassium-exchanging ATPase activity	15
Slfn8	Schlafen 8	Molecular function unknown	15
Casp11	Caspase 11, apoptosis-related cysteine protease	Cysteine-type peptidase activity	15
Nr1d1	Nuclear receptor subfamily 1, group D, member 1	Transcription factor activity	15
Ugt1a1	UDP-glucuronosyltransferase 1 family, member 1	Glucuronosyltransferase activity	15
Jcam2	Junction adhesion molecule 2	Integral to membrane	15
Car6	Carbonic anhydrase 6	Carbonate dehydratase activity; lyase activity; zinc ion binding	16
Ebi3	Epstein-Barr virus induced gene 3	Hematopoietin/interferon-class (D200-domain) cytokine receptor activity; interleukin-27 receptor binding	16

(*Table continues*)

Table 2. *Continued*

Up-regulated genes

Gene name	Gene description	GO molecular function/GO biological process/ GO cellular component	Fold change
Ebi3	Epstein-Barr virus induced gene 3	Hematopoietin/interferon-class (D200-domain) cytokine receptor activity; interleukin-27 receptor binding	16
Ms4a7	Membrane-spanning 4-domains, subfamily A, member 7	Unavailable annotation	16
C1qg	Complement component 1, q subcomponent, gamma polypeptide	Complement activation	16
BC032204	CDNA sequence BC032204	2′-phosphotransferase activity	16
CD 207 antigen	Langerin	Sugar binding	16
Fcgr3	Fc receptor, IgG, low-affinity Iib	IgG binding; IgG receptor activity	16
H2-D1	Histocompatibility 2, D region locus 1	MHC class I receptor activity	17
Gpnmb	Glycoprotein (transmembrane) nmb	Carbon-nitrogen ligase activity, with glutamine as amido-*N*-donor; heparin binding; integrin binding	17
Slpi	Secretory leukocyte protease inhibitor	Serine-type endopeptidase inhibitor activity	17
Ly86	Lymphocyte antigen 86	Inflammatory response	17
Kcnn4	Potassium intermediate/small conductance calcium-activated channel, subfamily N, member 4	Calcium-activated potassium channel activity; calmodulin binding	17
BC020152	RIKEN cDNA B930011D01 gene	Protein binding	17
Csf1r	Colony stimulating factor 1 receptor	Transmembrane receptor protein tyrosine kinase activity	17
Evi2a	Ecotropic viral integration site 2a	Extracellular space	17
Vav	vav 1 oncogene	Diacylglycerol binding; guanyl-nucleotide exchange factor activity	18
Slc1a6	Solute carrier family 1, member 6	Carrier activity; sodium:dicarboxylate symporter activity	18
Prg	Proteoglycan, secretory granule	Extracellular space	18
Cp	Ceruloplasmin	Ferroxidase activity	18
Msr1	Macrophage scavenger receptor 1	Lipid transporter activity; scavenger receptor activity	19
Pira6	Paired-Ig-like receptor A6	Receptor activity; sugar binding	19
Thbs4	Thrombospondin 4	Structural molecule activity	19
Nt5e	5′ nucleotidase, ecto	Hydrolase activity; hydrolase activity, acting on ester bonds	19
Itgb2	Integrin beta 2	Protein binding; receptor activity	19
BC027331	Pyrimidinergic receptor P2Y, G-protein coupled, 6	UDP-activated nucleotide receptor activity; pyrimidine nucleotide binding	19
LOC226421	RIKEN cDNA 5430435G22 gene	Carboxypeptidase A activity	19
Fyb	FYN-binding protein	Nucleus	19
Clecsf10	C-type (calcium-dependent, carbohydrate recognition domain) lectin, superfamily member 10	Sugar binding	19
Lpl	Lipoprotein lipase	Heparin binding; hydrolase activity; lipoprotein lipase activity	20
Cd68	CD68 antigen	Extracellular space	20
Lcp1	Lymphocyte cytosolic protein 1	Actin binding; calcium ion binding	20
Cpb1	Carboxypeptidase B1 (tissue)	Carboxypeptidase B activity	20
Icsbp	Interferon consensus sequence binding protein 1	Transcription factor activity	20
AA673245	RIKEN cDNA 2610028F08	transmembrane receptor protein tyrosine kinase activity	21
Cxcl10	Chemokine (C-X-C motif) ligand 10	Chemokine activity; cytokine activity	21
Tnfaip2	Tumor necrosis factor, alpha-induced protein 2	Angiogenesis, cell differentiation, development	21
Cxcl4	Chemokine (C-X-C motif) ligand 4	Chemokine activity; cytokine activity	21
BC026627	RIKEN cDNA D930038M13 gene	Extracellular space	21
AW557061	RIKEN cDNA 9030611N15 gene	Oxidoreductase activity	22
H2-L	Histocompatibility 2, D region	MHC class I receptor activity	22
Brdg1-pending	Expressed sequence AI586015	SH3/SH2 adaptor activity; protein binding	22
Hcph	Hemopoietic cell phosphatase	Hydrolase activity; prenylated protein tyrosine phosphatase activity	22
Ci1-pending	Solute carrier family 15, member 3	Transporter activity	22
Lrrc33	Leucine-rich repeat containing 33	Integral to membrane	22
Ms4a6d	Membrane-spanning 4-domains, subfamily A, member 6D	Unavailable annotation	22

(*Table continues*)

Table 2. *Continued*

Up-regulated genes

Gene name	Gene description	GO molecular function/GO biological process/ GO cellular component	Fold change
Ndr1	N-myc downstream regulated 1	Mast cell activation	22
Tyrobp	TYRO protein tyrosine kinase binding protein	Protein binding	23
Sp100	Nuclear antigen Sp100	DNA binding	23
Stab1	Stabilin 1	Hyaluronic acid binding; structural molecule activity	23
Laptm5	Lysosomal-associated protein transmembrane 5	Integral to membrane	23
Ccl9	Chemokine (C-C motif) ligand 9	Chemokine activity; cytokine activity	23
BC025893	Expressed sequence BB146404	Unavailable annotation	24
Adh7	Alcohol dehydrogenase 7 (class IV), mu or sigma polypeptide	Alcohol dehydrogenase activity, zinc-dependent; oxidoreductase activity	24
C1qa	Complement component 1, q subcomponent, alpha polypeptide	Complement activation, classical pathway	24
Comp	Histocompatibility 2, D region locus 1	MHC class I receptor activity	24
Cxcl5	Chemokine (C-X-C motif) ligand 5	Chemokine activity; cytokine activity	24
Ptprc	Protein tyrosine phosphatase, receptor type, C	Hydrolase activity; protein-tyrosine-phosphatase activity	25
Cd53	CD53 antigen	Antimicrobial humoral response	25
Prelp	Proline arginine-rich end leucine-rich repeat	Extracellular matrix structural constituent	25
Apobec1	Apolipoprotein B editing complex 1	Hydrolase activity; zinc ion binding	25
Clecsf8	C-type (calcium-dependent, carbohydrate recognition domain) lectin, superfamily member 8	Sugar binding	26
C1r	Complement component 1, r subcomponent	Chymotrypsin activity; hydrolase activity; serine-type endopeptidase activity	27
BC006623	RIKEN cDNA 1810046I24 gene	Receptor activity; sugar binding	27
Dock2	Dedicator of cyto-kinesis 2	Rac GTPase activator activity	27
Gp49b	Glycoprotein 49 B	Receptor activity	28
AI463083	RIKEN cDNA 4930568P13 Gene	Unavailable annotation	28
Rarres2	Retinoic acid receptor responder 2	Defense response	29
Csf2rb1	Colony stimulating factor 2 receptor	Hematopoietin/interferon-class (D200-domain) cytokine receptor activity	29
Bst1	Bone marrow stromal cell antigen 1	NAD+ nucleosidase activity; hydrolase activity	29
Lst1	Leukocyte-specific transcript 1	Cellular morphogenesis	31
Ccl3	Chemokine (C-C motif) ligand 3	Chemokine activity; cytokine activity	32
Pirb	Paired-Ig-like receptor B	Receptor activity	32
Fcer1g	Fc receptor, IgE, high affinity I, gamma polypeptide	IgE binding; IgG binding; receptor activity; transmembrane receptor activity	33
Adam23	A disintegrin and metalloprotease domain 23	Metalloendopeptidase activity	35
Mpeg1	Macrophage expressed gene 1	Unavailable annotation	35
Hp	Haptoglobin	Chymotrypsin activity; hemoglobin binding	37
Car9	Carbonic anhydrase 9	Carbonate dehydratase activity; lyase activity; zinc ion binding	38
Epsti1	Epithelial stromal interaction 1	Unavailable annotation	39
Msr1	Macrophage scavenger receptor 1	Lipid transporter activity; receptor activity; scavenger receptor activity	41
C1qr1	Complement component 1, q subcomponent, receptor 1	Calcium ion binding; protein binding;receptor activity; sugar binding	42
Fabp4	Fatty acid binding protein 4, adipocyte	Binding; lipid binding; transporter activity	43
Evi2b	Ecotropic viral integration site 2b	Integral to membrane	45
Ccl6	Chemokine (C-C motif) ligand 6	Chemokine activity; cytokine activity	45
Pfc	Properdin factor, complement	Complement pathway; immune response	47
Igsf6	Immunoglobulin superfamily, member 6	Integral to membrane	47
Xdh	Xanthine dehydrogenase	Xanthine dehydrogenase activity	48
Ncf1	Neutrophil cytosolic factor 1	Superoxide-generating NADPH oxidase activity	51
Ifi203	Interferon-activated gene 203	Immune response	53
Ifi202b	Interferon-activated gene 202B	Protein binding	53
Trem2b	Triggering receptor expressed on myeloid cells 2b	Receptor activity; transmembrane receptor activity	57
Psmb8	Proteosome subunit, beta type 8	Endopeptidase activity; hydrolase activity	57
BG066664	cDNA sequence BC032204	Cell adhesion molecule activity	58
Cd48	CD48 antigen	Extracellular space	59
Ifi205	Interferon-activated gene 205	Nucleic acid binding	64
Lyzs	Lysozyme	Hydrolase activity, acting on glycosyl bonds	64
Fgl2	Fibrinogenlike protein 2	Extracellular space	68
Casp1	Caspase 1	Caspase activity; cysteine-type peptidase activity	80
Fcgr2b	Fc receptor, IgG, low-affinity Iib	IgG binding; IgG receptor activity	80
Sod3	Superoxide dismutase 3, extracellular	Antioxidant activity; copper, zinc superoxide dismutase activity	85

(*Table continues*)

Table 2. *Continued*

Up-regulated genes

Gene name	Gene description	GO molecular function/GO biological process/ GO cellular component	Fold change
Pkib	Protein kinase inhibitor beta, cAMP dependent, testis specific	cAMP-dependent protein kinase inhibitor activity	105
Ifi27	Interferon, alpha-inducible protein 27	Unavailable annotation	112
Mmp13	Matrix metalloproteinase 13	Interstitial collagenase activity; metalloendopeptidase activity	126
Ibsp	Integrin-binding sialoprotein	Protein binding	241

Down-regulated genes

Gene name	Gene description	GO molecular function/GO biological process/ GO cellular component	Fold change
MEM46	Transmembrane protein 4	Integral to membrane	−10
Pitx2	Pairedlike homeodomain transcription factor 2	Transcription factor activity	−10
Nespas	Neuroendocrine secretory protein antisense	Unavailable annotation	−10
Nmyc1	Neuroblastoma myc−related oncogene 1	Transcription factor activity	−11
Ccni	Cyclin I	Cyclin-dependent protein kinase regulator activity	−11
Cd24a	CD24a antigen	External side of plasma membrane	−11
Ank1	Ankyrin 1, erythroid	Protein binding	−11
Sart3	Squamous cell carcinoma antigen recognized by T-cells 3	RNA binding	−11
Rxrg	Retinoid X receptor gamma	ligand-dependent nuclear receptor activity; steroid hormone receptor activity	−12
Gpr37	G protein-coupled receptor 37	G-protein coupled receptor activity; rhodopsin-like receptor activity	−12
Nipsnap1	4-nitrophenylphosphatase domain and non-neuronal SNAP25-like protein homolog 1 (*C. elegans*)	Mitochondrion	−12
Asb4	Ankyrin repeat and SOCS box-containing protein 4	DNA-binding; transcription factor activity	−13
Pcdh8	Protocadherin 8	Calcium ion binding; protein binding	−13
Fjx1	Four-jointed box 1 (*Drosophila*)	Unavailable annotation	−13
Ttn	Titin	Peroxidase activity; structural constituent of cytoskeleton	−13
Bex2	Brain expressed X-linked 2	Extracellular space	−14
Gdf5	Growth differentiation factor 5	Cytokine activity; growth factor activity; protein binding	−15
Peg3	Paternally expressed 3	Nucleic acid binding	−15
Tnnt1	Troponin T1, skeletal, slow	Structural constituent of cytoskeleton	−15
Sln	Sarcolipin	Enzyme regulator activity	−15
Astn1	Astrotactin 1	Protein binding	−15
Myod1	Myogenic differentiation 1	RNA polymerase II transcription factor activity, enhancer binding	−16
NM_026433	RIKEN cDNA 1810057C19 gene	Integral to membrane	−16
Myla	Myosin, light polypeptide 4	Calcium ion binding motor activity	−16
Chrna1	Cholinergic receptor, nicotinic, alpha polypeptide 1 (muscle)	Extracellular ligand-gated ion channel activity; nicotinic acetylcholine-activated cation-selective channel activity	−17
NM_025376	RIKEN cDNA 1110002H13 gene	Integral to membrane	−18
Igsf9	Immunoglobulin superfamily, member 9	Dendrite morphogenesis	−19
Acta1	Actin, alpha 1, skeletal muscle	Motor activity; structural constituent of cytoskeleton; structural molecule activity	−19
Pde9a	Phosphodiesterase 9A	3′,5′-cyclic-nucleotide phosphodiesterase activity; cGMP-specific phosphodiesterase activity; catalytic activity; hydrolase activity; manganese ion binding	−20
Mybph	Myosin-binding protein H	Protein binding	−21
Sema6a	Sema domain, transmembrane domain (TM), and cytoplasmic domain, (semaphorin) 6A	Receptor activity	−21
Sox11	SRY-box containing gene 11	DNA binding; transcription factor activity	−21
Lrp4	Low-density lipoprotein receptor-related protein 4	Chymotrypsin activity; hydrolase activity; scavenger receptor activity; serine-type endopeptidase activity; transmembrane receptor activity	−22
Kcnd2	Potassium voltage-gated channel, Shal-related family, member 2	Voltage-gated potassium channel activity	−22
Il17b	Interleukin 17B	Cytokine activity; protein binding; receptor binding	−22
Gcat	Glycine C-acetyltransferase (2-amino-3-ketobutyrate-coenzyme A ligase)	Acyltransferase activity; ligase activity; transaminase activity	−22
Sostdc1	sclerostin domain containing 1	Protein binding	−22

(*Table continues*)

Table 2. *Continued*

Down-regulated genes

Gene name	Gene description	GO molecular function/GO biological process/ GO cellular component	Fold change
Siat7c	Sialyltransferase 7 ((alpha-*N*-acetylneuraminyl 2,3-betagalactosyl-1,3)-*N*-acetyl galactosaminide alpha-2,6-sialyltransferase) C	Sialyltransferase activity	−24
BC005730	RIKEN cDNA A330049M08 gene	Unavailable annotation	−26
Cacna1s	Calcium channel, voltage-dependent, L-type, alpha 1S subunit	Voltage-gated calcium channel activity	−26
Tnni2	Troponin I, skeletal, fast 2	Actin-binding; hydrogen-exporting ATPase activity; structural constituent of cytoskeleton	−26
Bcl11a	B-cell CLL/lymphoma 11A (zinc finger protein)	Nucleic acid binding; transcription corepressor activity	−26
Prom1	Prominin 1	Phototransduction	−26
Hba-a1	Hemoglobin alpha, adult chain 1	Oxygen binding; oxygen transporter activity	−28
Mb	Myoglobin	Oxygen transporter activity	−28
Grip1	Glutamate receptor-interacting protein 1	Protein binding	−29
Tncc	Troponin C, cardiac/slow skeletal	Calcium ion binding; structural constituent of cytoskeleton	−30
Chrng	Cholinergic receptor, nicotinic, gamma polypeptide	Neurotransmitter receptor activity; nicotinic acetylcholine-activated cation-selective channel activity	−36
Casq2	Calsequestrin 2	Calcium ion binding; calcium ion storage activity	−38
Actn2	Actinin alpha 2	Actin-binding; actin filament binding; calcium ion binding; protein binding, bridging	−38
Nnat	Neuronatin	Actin binding; actin filament binding; calcium ion binding; protein binding, bridging	−40
Bmp7	Bone morphogenetic protein 7	Cytokine activity; growth factor activity; protein binding	−40
Actc1	Actin, alpha, cardiac	Motor activity; structural constituent of cytoskeleton	−42
Dusp9	Dual specificity phosphatase 9	Kinase activity phosphoprotein phosphatase activity	−43
Dcx	Doublecortin	Microtubule binding; protein binding	−44
Rex3	Reduced expression 3	Protein binding	−50
AV271892	RIKEN cDNA 4931417E21 gene	Mitochondrion	−53
Lrrn1	Leucine-rich repeat protein 1, neuronal	Extracellular space	−84
Myog	Myogenin	DNA binding; RNA polymerase II transcription factor activity, Enhancer binding	−85
Tnnt2	Troponin T2, cardiac	Structural constituent of cytoskeleton	−98
Tnni1	Troponin I, skeletal, slow 1	Actin binding; structural constituent of cytoskeleton	−111
Mylpf	Myosin light chain, phosphorylatable, fast skeletal muscle	Calcium ion binding	−141
Tncs	Troponin C2, fast	Calcium ion binding, structural constituent of cytoskeleton	−245
Hbb-y	Hemoglobin Y, betalike embryonic chain	Oxygen binding, oxygen transporter activity	−254
Myh3	Myosin, heavy polypeptide 3, skeletal muscle, embryonic	ATP-binding; actin binding	−392
Mylf	Myosin, light polypeptide 1	Calcium ion binding	−339

culture and are subsequently down-regulated (represented by *Crtl1*; Figure 5B, left panel). Cluster 3 contained 119 probe sets that are down-regulated during the time course (e.g., *Myod1*; Figure 5C, left panel). Additional probe sets demonstrating these expression profiles for each cluster are shown in Figure 5 (right panels).

The K-means clustering algorithm was subsequently used to reduce the numbers of genes assigned to each group and to identify the most correlated probe sets in a given cluster. The resulting clusters contained subsets of probes that were most similar to cluster 1, 2, and 3, and contained 21, 12, and 23 probe sets, respectively (Figure 5). All 21 transcripts identified in cluster 1, and 10 of the 23 probe sets found in cluster 3 were identified in the group of 10-fold up- and down-regulated genes, respectively (see Table 2). Cluster 1 genes include other matrix molecules such a *Ibsp* and cartilage oligomeric protein (*Comp*), which are documented chondrogenic markers (Figure 5A). Additional components of the cartilage extracellular matrix were identified in cluster 2 (Figure 5B). Among the expressed transcripts were *Col2a1* and the newly implicated angiotensin II receptor, type 2 (*Agtr2*), a G-protein-coupled receptor involved in regulating collagen expression in cardiac myocytes (Ma *et al.*, 1998). Cluster three represented many myogenic markers such as cardiac actin (*Actc1*) and troponin T1 (*Tnnt1*), a gene thought to be involved in muscle contractility that are all down-regulated as chondrocytes differentiate (Figure 5C). Genes in cluster 3 (as well as other genes that are down-regulated early in micromass differentiation) are therefore likely due to the suppression of nonchondrogenic cell lineages (such as myoblasts) under the culture conditions used.

Functional Validation of Microarray Results: Rgs2 Regulates Chondrocyte Differentiation

One pervasive expression pattern identified with cluster analysis of the microarray data set included genes that are

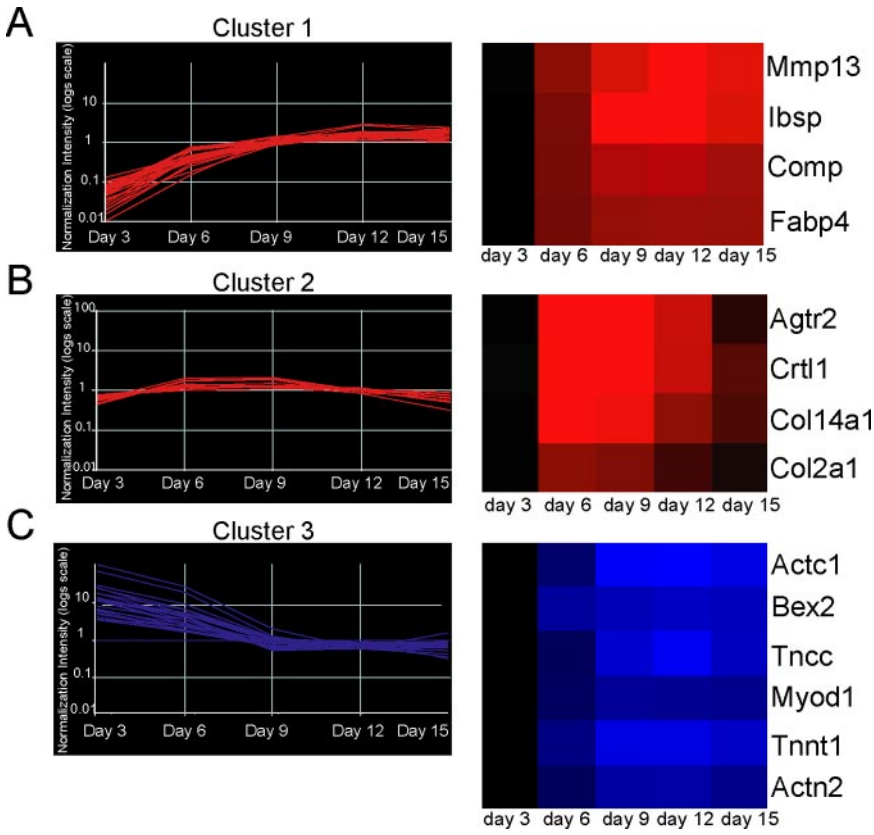

Figure 5. Self-organizing maps and k-means clustering of microarray data. SOM analysis of 3334 probe sets from GeneSpring analysis and subsequent k-means clustering of three SOM derived clusters. Cluster 1 contains genes that show up-regulation toward day 15 of the micromass time course (A, left panel). Genes in this cluster include *Mmp13*, *Ibsp*, *Comp*, and fatty acid binding protein 4 (*Fabp4*; A, right panel). Standard correlation was used to measure similarity between expression profiles. Cluster 2 contains genes following an expression pattern similar to that of Cartilage link protein (*Crtl1*; B, left panel), such as Angiotensin II receptor type 2 (*Atgr2*), collagen 14 (*Col14a1*), and *Col2a1* (B, right panel). Cluster 3 represents the expression pattern of genes down-regulated over time (C, left panel), including cardiac actin (*Actc1*), brain expressed X-linked 2 (*Bex2*), *Tncc*, *Myod1*, troponin (*Tnnt1*), and alpha actinin (*Actn2*; C, right panel). Red lines show up-regulation and blue lines show down-regulation of gene expression.

up-regulated as micromass cultures approach the end of their development program. We postulated that genes following this particular expression pattern might promote chondrocyte maturation. *Rgs2* was among the probe sets that exhibit this expression pattern. *Rgs2* transcripts increased by twofold as the micromass cultures progressed from day 3 to day 12 of culture and dropped slightly thereafter (Figure 6A). Semiquantitative RT-PCR confirmed that *Rgs2* was indeed markedly up-regulated during micromass culture; however, the drop in *Rgs2* expression at day 15 of culture was not observed in these experiments, potentially due to slight variations in the amounts of RNA or cDNA as shown by *Actin* RT-PCR (Figure 6B). To clarify the expression pattern of *Rgs2* in growth plate cartilage in vivo, we performed in situ hybridization on tibia sections from E15.5 mice (Figure 6C). *Rgs2* expression was weak in resting chondrocytes, increased markedly in proliferating and in prehypertrophic chondrocytes, and decreased upon full hypertrophic differentiation. These in vivo data thus confirm the expression patterns observed in microarray analyses of micromass cultures.

We stably transfected an HA-tagged human RGS2 expression vector into the chondrogenic cell line ATDC5 (Atsumi *et al.*, 1990) and differentiated them for 18 d to further investigate the role of RGS2 expression in chondrocyte differentiation. Overexpression of RGS2 was confirmed by 1) RT-PCR using primers designed against the N-terminal HA-tag and the RGS2 coding region, and 2) Western blotting using an anti-HA antibody. Both RGS2 mRNA and protein were elevated compared with cells expressing the control vector and generated a 657-base pairs amplicon and 32-kDa protein, respectively (Figure 6D).

On examination of chondrocyte phenotype, we found that RGS2 overexpression causes increased glycosaminoglycan synthesis (as shown by a more rapid increase in the intensity of Alcian blue staining; Figure 7A) and ALP activity, both in staining (Figure 7B) and enzymatic assays (Figure 7C). Real-time PCR analysis of the culture for stage-specific cartilage markers reveal no significant differences in the levels of *Sox9*, *Col2a1,* and *Ihh* transcripts in cells overexpressing *Rgs2* compared with control cultures (Figure 8, A, B, and D). The expression of two other markers of chondrocyte differentiation, *Fgfr3* and *Ibsp*, however, is increased by ~2- and 10-fold, respectively in these cultures (Figure 8, C and E). The accelerated increase in glycosaminoglycan synthesis, ALP activity, and *Fgfr3* and *Ibsp* expression suggest that overexpression of RGS2 accelerates the rate of chondrocyte differentiation and modulates the expression of certain markers of the chondrocyte phenotype, thus confirming the roles postulated from the microarray expression pattern.

DISCUSSION

Recent studies in our lab and other labs have established the micromass culture system as a reliable model of chondrogenic differentiation in primary mammalian cells (Weston *et al.*, 2000; Cormier *et al.*, 2003; Stanton *et al.*, 2004; Zhang *et al.*, 2004). Initially, cells condense in a population of pluripotent mesenchymal cells that subsequently differentiate along the chondrogenic lineage. Here we confirmed authentic chondrogenic differentiation over time using staining techniques and assessing molecular markers. We then performed microarray analyses to identify gene expression patterns and novel regulators of cartilage development. In silico analysis of microarray data demonstrate expected expression patterns for numerous known cartilage markers. Examples include the transient upregulation of the genes encoding the cartilage marker proteins collagen 2, aggrecan, link protein,

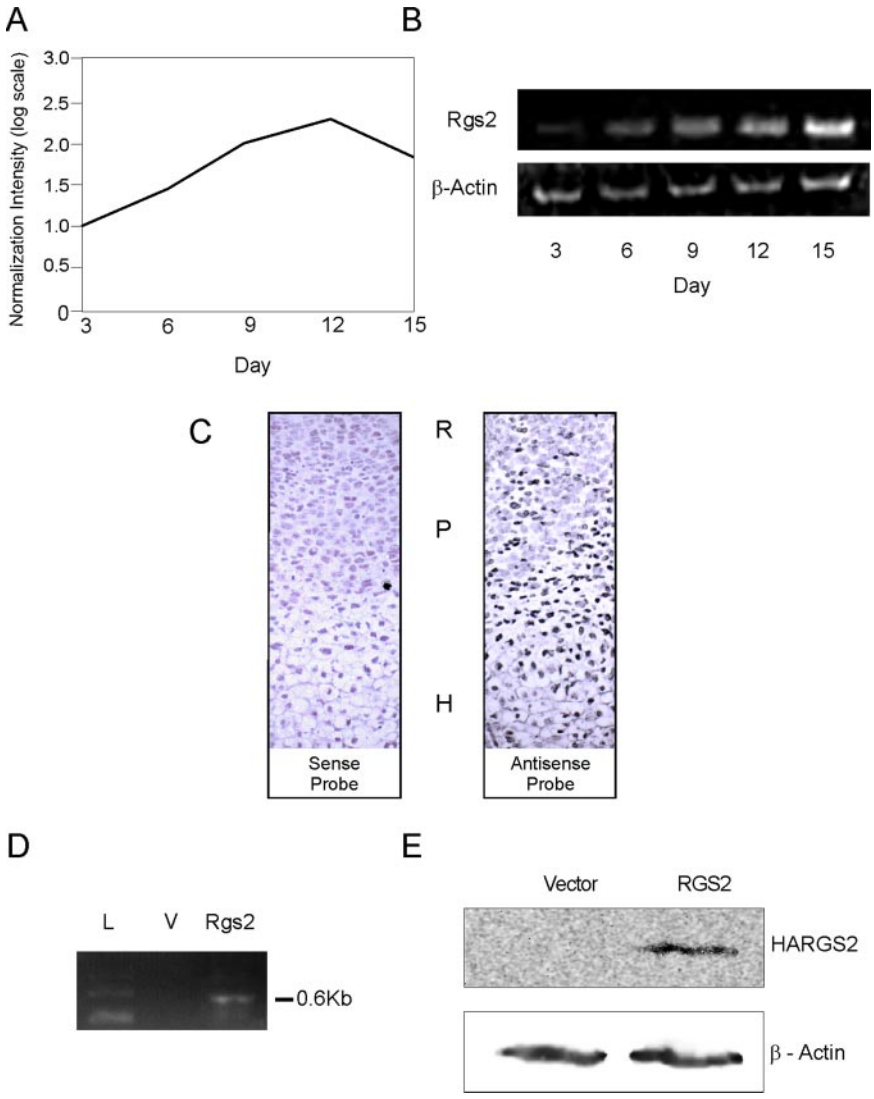

Figure 6. Confirmation of *Rgs2* expression in murine chondrocyte differentiation. Microarray expression pattern for *Rgs2* in micromass cultures show transcript accumulation from days 3 to 12 of culture, with a subsequent drop in expression (A). *Rgs2* mRNA up-regulation during micromass differentiation was confirmed by RT-PCR using β-actin as a loading control (B). *Rgs2* mRNA expression in the tibia of a E15.5 mouse was analyzed by in situ hybridization (C). Sense probes resulted in no signal, whereas *Rgs2* antisense probes demonstrated weak or no expression in resting chondrocytes (R), strong expression of *Rgs2* mRNA in proliferating (P) and prehypertrophic chondrocytes, and lower expression in fully hypertrophic chondrocytes (H). Confirmation of RGS2 overexpression in chondrogenic ATDC-5 cells by RT-PCR and Western blotting (C). Ladder (L), pcDNA 3.1+ vector (V), and a 657-bp Rgs2 amplicon are shown (left panel). Cell lysates isolated from ATDC-5 cells overexpressing HA-tagged RGS2 were separated by SDS-PAGE and blotted onto nitrocellulose membrane, which was subsequently probed with an anti-HA antibody (right panel).

and Cd-Rap, and the late and strong induction of *Mmp13* and *Ibsp* genes. Similarly, myogenic markers such as *Myod1* are rapidly and strongly down-regulated in culture, consistent with stimulation of chondrogenic differentiation and suppression of myogenic differentiation in our micromass culture system (Weston *et al.*, 2003). Genes in cluster 3, such as *Myod1*, that are down-regulated early in micromass differentiation therefore most likely represent the suppression of other cell lineages (e.g., the myogenic lineage) in our culture system, rather than the selective down-regulation of these genes during differentiation within the chondrocyte lineage.

In addition to demonstrating the expected expression patterns of established differentiation markers, microarray data were validated using real-time and RT-PCR analyses for several genes, as well as by in situ hybridization of tissue sections for *Rgs2*. All these results demonstrate that expression patterns observed in the microarray experiments of micromass cultures reflect authentic expression in vitro and in vivo, at least for the vast majority of genes.

The functional distribution of GO-annotated probe sets identified using different fold change cutoffs was similar. Strongly represented categories included probe sets involved in catalysis and signal transduction. A large proportion of unannotated genes were also identified, suggesting that additional novel chondrogenic markers or markers that have not been implicated in chondrocyte differentiation exist and warrant further investigation. This analysis presents an additional avenue from which candidate genes can be categorized and analyzed. Comparisons between genes expressed on day 3 and day 15 of micromass culture that were filtered with a minimum twofold change cutoff produced a list containing 1772 genes. Numerous gene families that have been implicated in different cellular processes were shown, some of which were unique to a particular expression pattern (up- or down-regulated). For example, several myogenic markers including *Myod1*, myosins, myogenin, and troponins demonstrate strongest down-regulation over time in micromass culture.

Analysis of the filtered data set shows that changes in gene expression accumulate from day 3 to day 15 of culture, so that the largest changes are observed when data sets from these culture days were compared, irrespective of the fold change cutoff used. This trend is consistent with the changes observed in the development of an organ system in which cells undergo a transition from a state of developmental plasticity to a state of determination, specification, and ultimately terminal differentiation (Loebel *et al.*, 2003). The larg-

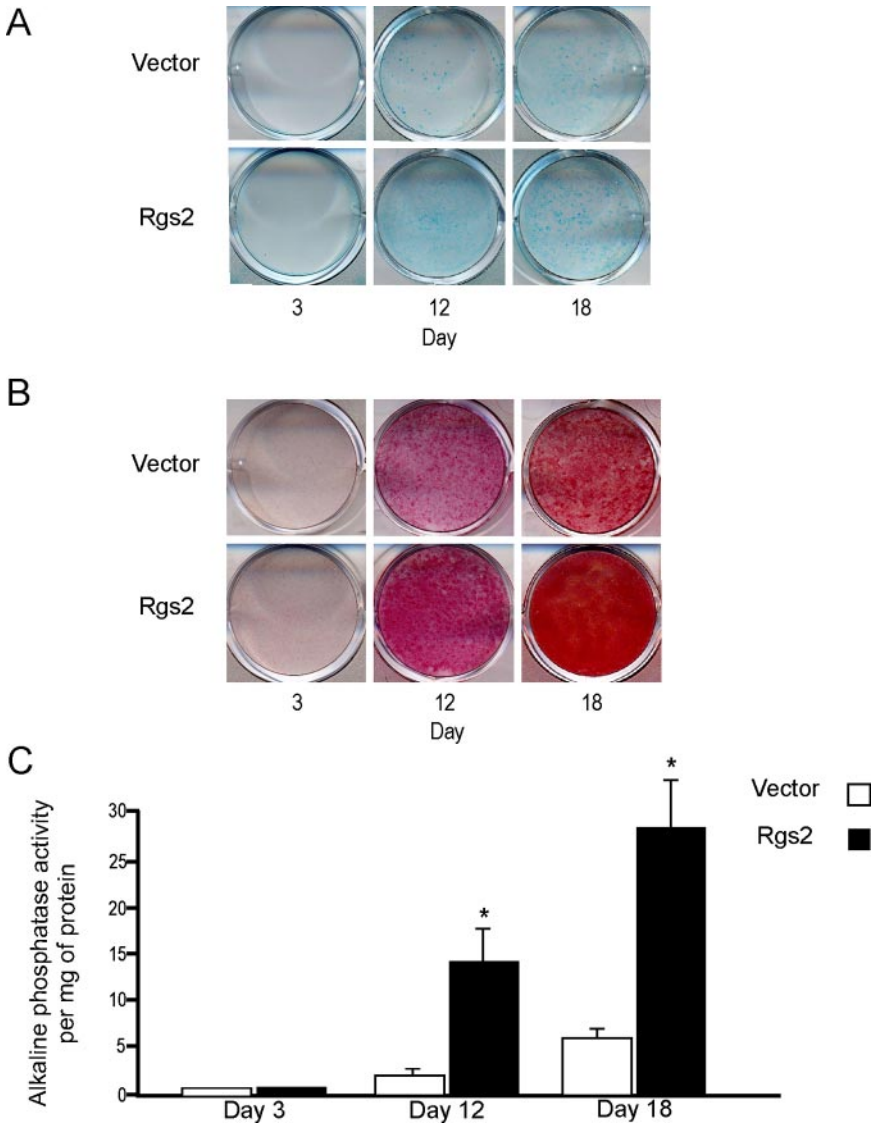

Figure 7. Functional characterization of RGS2 in chondrocyte differentiation. Differentiating ATDC-5 cells stably overexpressing RGS2 were stained with Alcian blue (A) and ALP on days 3, 12, and 18 of culture (B). ALP activity was subsequently quantified by enzyme assay. Stainings were repeated three times on independent trials, and ALP activity values represent an average of six independent trials. Significant differences from the vector control (***) were determined by $p < 0.001$. RGS2 overexpression results in accelerated and increased induction of glycosaminoglycan synthesis and ALP activity.

est successive changes in gene expression occur between days 3 and 6 of the culture period, which is consistent with chondrogenic differentiation. Changes observed between the later developmental stages were conversely smaller.

A caveat of microarray analysis is the generation of data sets with high dimensionality, which in turn generates a proportion type I errors (Dudoit and Fridlyand, 2002; Reiner *et al.*, 2003). Microarray analysis is also limited in its ability to quantify the expression levels observed for any given chip (Sekiya *et al.*, 2002; Barash *et al.*, 2004). These two features pose a problem with interpreting the significance of expression data. Currently, studies are underway to bypass these obstacles; however, a consensus has yet to be reached regarding the selection of optimal normalization algorithms in particular (Love *et al.*, 2002). M.A.S. 5.0 algorithm from Affymetrix, Model Based Expression Index (Li and Wong, 2001) and Robust Multi-array analysis (RMA; Irizarry *et al.*, 2003) are examples of currently used summary measures. In our case we processed the data according to MAS 5.0 algorithms and subsequently filtered the data in both GeneSpring 6.1 and in GeneTraffic 3.0, which used RMA. A range of filtering parameters (i.e., 2-, 5- and 10-fold change cutoffs) was also used to identify the distribution and the degree to which the expression of certain genes change.

Higher stringency normalization and filtering reduces the frequency of false positive data, because noise is dependent on the observed signal intensity (Tu *et al.*, 2002; Cole *et al.*, 2003). We must establish a balance between excluding biologically meaningful data by using restrictive analysis criteria and using permissive parameters, which could likewise reduce the biological value of the data by increasing the number of artifacts. For example, normalization and analysis of our data set in GeneSpring identified the temporal expression pattern of *Rgs2*, whereas changes in *Rgs2* mRNA expression were not deemed significant using the more stringent RMA normalization in GeneTraffic. However, confirmation of the *Rgs2* expression with RT-PCR suggests that normalization and subsequent filtering of the data in GeneSpring produces biologically relevant data sets. Similar findings were also obtained with numerous other genes (unpublished data).

At the same time, however, the larger gene lists generated in GeneSpring make the selection of a manageable number of candidate molecules for functional characterization a

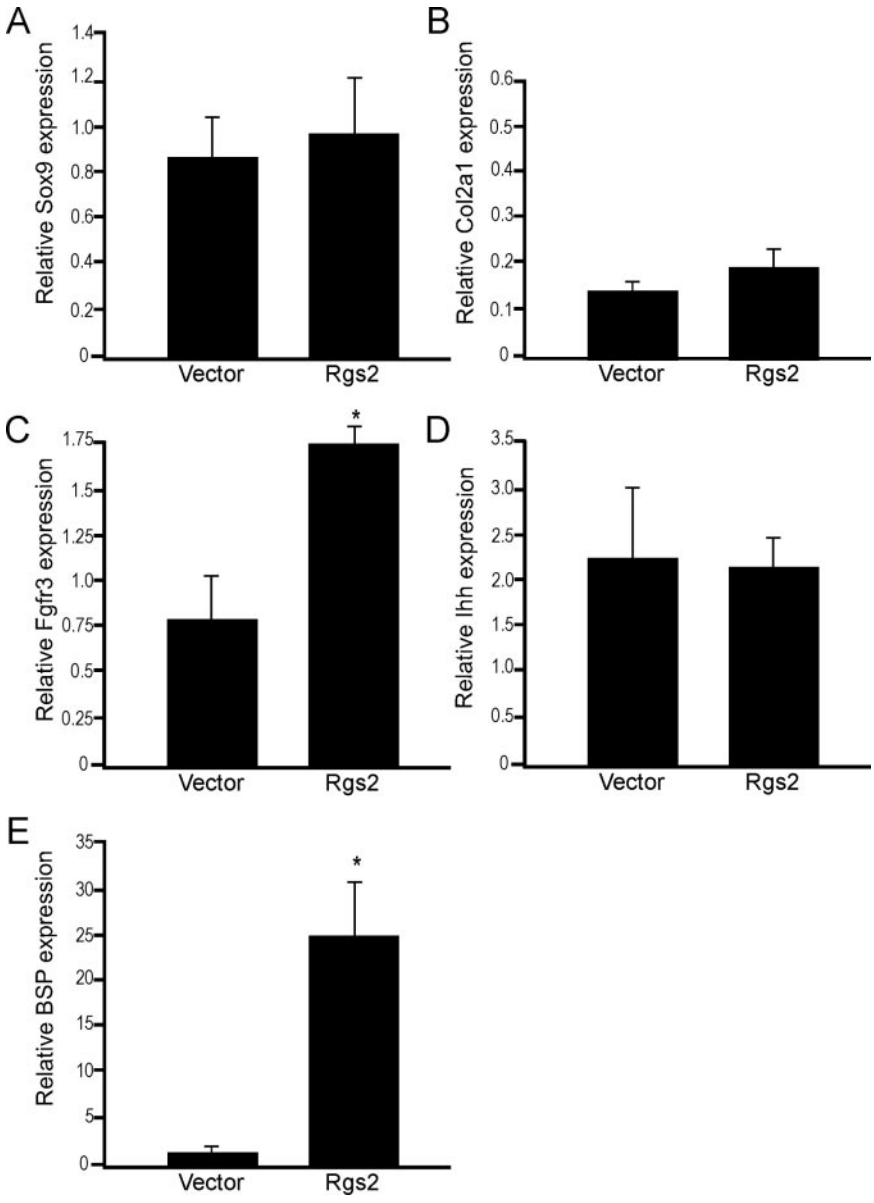

Figure 8. Effects of RGS2 overexpression on chondrocyte gene expression. The relative abundance of *Sox9* (A), *Col2a1* (B), *Fgfr3* (C), *Ihh* (D), and *Ibsp* (E) transcripts in ATDC-5 cells overexpressing RGS2 was quantified with real-time PCR. Expression of *Sox9* and *Col2a1* were assessed after 6 d of culture and the expression of all subsequent markers assessed on day 15 of culture. Results represent means and standard deviations from three independent trials completed in triplicate. Expression values are normalized to a *Gapdh* internal control. Significant differences in expression from control (*) were determined by $p < 0.001$.

much more complex task. It is important to note that the gene expression patterns observed in the data set are similar between both analysis methods, i.e., GeneSpring versus GeneTraffic. Furthermore, the probe sets identified by parallel filtering methods show the expected inverse correlation between the number of identified probe sets and the fold change cutoff used. For example, the myogenic markers identified in this list are consistently down-regulated in both programs even though GeneSpring analysis proves to be less stringent. These findings highlight the fine balance between the specificity and sensitivity of normalization algorithms and filtering conditions, and the importance of implementing algorithms that coincide with the biological questions of interest. Combining robust statistical algorithms with various filtering stringencies provides a broader spectrum of changes from which integrative hypotheses may be derived while maintaining both the statistical confidence and biological relevance of the analyzed expression data.

Our cluster analyses revealed numerous groups of coexpresssed genes, three of which were analyzed in more detail. The probe sets identified in cluster 1 contained *Mmp13* as well as probe sets for genes exhibiting a minimum 10-fold up-regulation from day 3 to 15 of micromass culture. Specifically, this cluster included other matrix molecules such as *Comp* and factors that have not been well characterized in the context of chondrogenic differentiation. Similarly, a group of CC and CXC chemokine receptors (CCRs) were identified in cluster 3 (Table 3). Silvestri *et al.* (2003) established the role of chemokine receptors in the maintenance of healthy cartilage by maintaining the balance between catabolic and anabolic processes in the tissues. Alaaeddine *et al.* (2001) demonstrated that chemokine receptor genes (CCRs) are up-regulated in human osteoarthritic. It is interesting to note that, contrary to the pattern observed for CCRs, several of their ligand chemokines exhibited a minimum 10-fold increase in gene expression during micromass differentiation in our data sets. This family of molecules has been

Table 3. RT-PCR primer sequences

Target	Primer sequences
β-actin	F: 5′-CACCCTGTGCTGCTCACCGAGGCC-3′ R: 5′-CCACACAGATGACTTGCGCTCAGG-3′
Cartilage link protein (Crtl-1)	F: 5′-GCA TCA AGT GGA CCA AGC TA-3′ R: 5′-GTA ACT CCA ATG CCA CCA CA-3`′
Myogenic differentiation 1 (Myod-1)	F: 5′-GCT CTG ATG GCA TGA TGG AT-3′ R: 5′-CCT GTT CTG TGT CGC TTA GG-3′
Nuclear cap binding protein subunit 2 (Ncbp2)	F: 5′-TAC GTG GAA CTC AGC GAG TA-3′ R: 5′-CTT GGA CCG CGA CCT AGA CT-3′
Regulator of G-protein signalling (Rgs2)	F: 5′-TGG ACA AGA GTG CAG GCA AC-3′ R: 5′-GTG AAG CAG CCA CTT GTA GC-3′
HA-tagged regulator of G-protein signalling (Rgs2)	F: 5′-GCT TAC CCA TAC GAT GTT CAA-3′ R: 5′-TGA GGC TCT GTG GTG ATT TG-3′

implicated in promoting chondrocyte hypertrophy (Merz *et al.*, 2003). Further studies should elucidate the roles chemokine receptors play in both normal and pathological cartilage conditions. Novel factors were also identified with the cluster analysis (Table 4). For example, the angiotensin type II receptor (*Agtr2*) (Ma *et al.*, 1998) exhibited an expression pattern similar to cartilage link protein and was found in cluster 2.

The activation of signaling cascades essential to endochondral bone growth and remodeling occurs partially through the coordinate action of G-protein-coupled receptors (GPCRs) and heterotrimeric G-proteins, for example, the parathyroid hormone and parathyroid hormone-related peptide receptor (PTH/PTHrP-R) and Gα subunit proteins (Bringhurst *et al.*, 1993; Bowler *et al.*, 1998; Chung *et al.*, 1998; Inoue and Matsumoto, 2000). Signaling through GPCRs is regulated by the activities of regulators of G-protein signaling (RGS) proteins, which are a family of signaling molecules implicated in regulating the rate at which G-proteins hydrolyze bound GTP (Hepler, 1999; De Vries *et al.*, 2000; Hepler, 2003; Ishii and Kurachi, 2003). RGS2 has been implicated in the down-regulation of PTH-mediated signaling in osteoblasts (Ko *et al.*, 2001; Thirunavukkarasu *et al.*, 2002). Our data suggest that the gene encoding RGS2 is also expressed in chondrocytes and functions in the regulation of chondrocyte differentiation in ATDC5 cells. RGS2 overexpression in these cultures advanced the production of glycosaminoglycans and ALP. Parallel increases in the expression of the chondrogenic marker genes *Fgfr3* and *Ibsp*, which to our knowledge have not yet been described as RGS2 target genes, were also observed. However, other chondrocyte markers, such as *Sox9* and *Indian hedgehog*, were not affected by RGS2 overexpression, suggesting that the effects of RGS2 are specific to certain aspects of chondrocyte maturation. Future studies will include in depth analysis of the mechanism of RGS2 regulation of chondrocyte differentiation. Nevertheless, these studies provide an example how our microarray analyses result in the identification of novel candidate regulators of chondrocyte differentiation and in the subsequent experimental validation of the hypothesized biological roles of these candidates.

Table 4. Cluster analysis

Cluster 1	Cluster 2	Cluster 3
Lpl	Agtr2	Actc1
Prelp	Crtl1	Mcam
C1r	Aass	Tbc1d8
Mmp13	Prlr	Bex2
Ibsp	Crtl1	Tnnc2
Cp	C230093N12Rik	Tncc
Sod3	Col14a1	Tpd52l1
Cxcl10	BC020108	Myod1
NM_134072	Bklhd2	Bmp7
Wisp2	Mglap	1110002H13Rik
Comp	Col2a1	Mybph
Adh7	Cnnm2	Tnnt1
Fgl2		Prom1
AI838132		Chrnb1
BC025893		Myl4
Car9		Trfr
BC026627		Acta1
Kcnn4		Rex3
Ndr1		Actn2
Fabp4		Pdlim3
BG067392		Tnnt3
		Tnni1
		Mb
		Art1

The integration of an in vitro limb culture system and high throughput microarray analysis has provided a valuable tool for identifying global gene expression profiles of markers and potential regulators of chondrogenic differentiation. Functional studies confirmed the biological relevance of the *Rgs2* expression pattern identified in our microarray analyses. This research facilitates the development of novel complex, testable hypotheses regarding potential regulators of chondrocyte development. These data thus provide the basis for improved understanding of cartilage development, homeostasis, and disease.

Note added in proof. All data sets have been submitted to the NCBI/GEO database (entry number GSE2154).

ACKNOWLEDGMENTS

Work in the laboratory of F.B. is supported by grants from the Canadian Institutes of Health Research, the Arthritis Society, the Canadian Arthritis Network, the Canada Research Chair Foundation, the National Science and Engineering Research Council, and the Hospital for Sick Children Foundation. C.G.J. is the recipient of an Ontario Graduate Scholarship in Science and Technology and a Canadian Institutes of Health Research Doctoral Award, and C.T.G.A. was supported by a stipend from the Ontario Genomics Institute.

REFERENCES

Ahrens, P. B., Solursh, M., and Reiter, R. S. (1977). Stage-related capacity for limb chondrogenesis in cell culture. Dev. Biol. *60*, 69–82.

Akiyama, H., Chaboissier, M. C., Martin, J. F., Schedl, A., and de Crombrugghe, B. (2002). The transcription factor Sox9 has essential roles in successive steps of the chondrocyte differentiation pathway and is required for expression of Sox5 and Sox6. Genes Dev. *16*, 2813–2828.

Al-Shahrour, F., Diaz-Uriarte, R., and Dopazo, J. (2004). FatiGO: a web tool for finding significant associations of gene ontology terms with groups of genes. Bioinformatics *20*, 578–580.

Alaaeddine, N., Olee, T., Hashimoto, S., Creighton-Achermann, L., and Lotz, M. (2001). Production of the chemokine RANTES by articular chondrocytes and role in cartilage degradation. Arthritis Rheum. *44*, 1633–1643.

Atsumi, S., Umezawa, K., Iinuma, H., Naganawa, H., Nakamura, H., Iitaka, Y., and Takeuchi, T. (1990). Production, isolation and structure determination of a novel beta-glucosidase inhibitor, cyclophellitol, from *Phellinus* sp. J. Antibiot. (Tokyo) *43*, 49–53.

Ballock, R. T., and O'Keefe, R. J. (2003). Physiology and pathophysiology of the growth plate. Birth Defects Res. Part C Embryo Today *69*, 123–143.

Barash, Y., Dehan, E., Krupsky, M., Franklin, W., Geraci, M., Friedman, N., and Kaminski, N. (2004). Comparative analysis of algorithms for signal quantitation from oligonucleotide microarrays. Bioinformatics *20*, 839–846.

Beier, F., Lee, R. J., Taylor, A. C., Pestell, R. G., and LuValle, P. (1999). Identification of the cyclin D1 gene as a target of activating transcription factor 2 in chondrocytes. Proc. Natl. Acad. Sci. USA *96*, 1433–1438.

Bi, W., Deng, J. M., Zhang, Z., Behringer, R. R., and de Crombrugghe, B. (1999). Sox9 is required for cartilage formation. Nat. Genet. *22*, 85–89.

Bowler, W. B., Gallagher, J. A., and Bilbe, G. (1998). G-protein coupled receptors in bone. Front Biosci. *3*, D769–D780.

Bringhurst, F. R., Juppner, H., Guo, J., Urena, P., Potts, J. T., Jr., Kronenberg, H. M., Abou-Samra, A. B., and Segre, G. V. (1993). Cloned, stably expressed parathyroid hormone (PTH)/PTH-related peptide receptors activate multiple messenger signals and biological responses in LLC-PK1 kidney cells. Endocrinology *132*, 2090–2098.

Cancedda, R., Castagnola, P., Cancedda, F. D., Dozin, B., and Quarto, R. (2000). Developmental control of chondrogenesis and osteogenesis. Int. J. Dev. Biol. *44*, 707–714.

Cancedda, R., Descalzi Cancedda, F., and Castagnola, P. (1995). Chondrocyte differentiation. Int. Rev. Cytol. *159*, 265–358.

Cash, D. E., Bock, C. B., Schughart, K., Linney, E., and Underhill, T. M. (1997). Retinoic acid receptor alpha function in vertebrate limb skeletogenesis: a modulator of chondrogenesis. J. Cell Biol. *136*, 445–457.

Cheah, K. S., Lau, E. T., Au, P. K., and Tam, P. P. (1991). Expression of the mouse alpha 1(II) collagen gene is not restricted to cartilage during development. Development *111*, 945–953.

Chen, J., Shapiro, H. S., and Sodek, J. (1992). Development expression of bone sialoprotein mRNA in rat mineralized connective tissues. J Bone Miner. Res. *7*, 987–997.

Chung, U. I., Lanske, B., Lee, K., Li, E., and Kronenberg, H. (1998). The parathyroid hormone/parathyroid hormone-related peptide receptor coordinates endochondral bone development by directly controlling chondrocyte differentiation. Proc. Natl. Acad. Sci. USA *95*, 13030–13035.

Cole, S.W.G., Galic, Z., and Zack, J. A. (2003). Controlling false-negative errors in microarray differential expression analysis: a PRIM approach. Bioinformatics *19*, 1808–1816.

Cormier, S. A., Mello, M. A., and Kappen, C. (2003). Normal proliferation and differentiation of Hoxc-8 transgenic chondrocytes in vitro. BMC Dev. Biol. *3*, 4.

De Vries, L., Zheng, B., Fischer, T., Elenko, E., and Farquhar, M. G. (2000). The regulator of G protein signaling family. Annu. Rev. Pharmacol. Toxicol. *40*, 235–271.

DeLise, A. M., Fischer, L., and Tuan, R. S. (2000). Cellular interactions and signaling in cartilage development. Osteoarthritis Cartilage *8*, 309–334.

Dietz, U. H., and Sandell, L. J. (1996). Cloning of a retinoic acid-sensitive mRNA expressed in cartilage and during chondrogenesis. J. Biol. Chem. *271*, 3311–3316.

Dudoit, S., and Fridlyand, J. (2002). A prediction-based resampling method for estimating the number of clusters in a dataset. Genome Biol. *3*, RESEARCH0036.

Eames, B. F., de la Fuente, L., and Helms, J. A. (2003). Molecular ontogeny of the skeleton. Birth Defects Res. Part C Embryo Today *69*, 93–101.

Eyre, D. R. (2004). Collagens and cartilage matrix homeostasis. Clin. Orthop. *427* (suppl), S118–S122.

Fang, C., Carlson, C. S., Leslie, M. P., Tulli, H., Stolerman, E., Perris, R., Ni, L., and Di Cesare, P. E. (2000). Molecular cloning, sequencing, and tissue and developmental expression of mouse cartilage oligomeric matrix protein (COMP). J. Orthop. Res. *18*, 593–603.

Gelse, K., Soder, S., Eger, W., Diemtar, T., and Aigner, T. (2003). Osteophyte development—molecular characterization of differentiation stages. Osteoarthritis Cartilage *11*, 141–148.

Hall, B. K., and Miyake, T. (1992). The membranous skeleton: the role of cell condensations in vertebrate skeletogenesis. Anat. Embryol. (Berl.) *186*, 107–124.

Hepler, J. R. (1999). Emerging roles for RGS proteins in cell signaling. Trends Pharmacol. Sci. *20*, 376–382.

Hepler, J. R. (2003). RGS protein and G protein interactions: a little help from their friends. Mol. Pharmacol. *64*, 547–549.

Inoue, D., and Matsumoto, T. (2000). Parathyroid hormone-related peptide and bone: pathological and physiological aspects. Biomed. Pharmacother. *54*(Suppl 1), 32s–41s.

Irizarry, R. A., Hobbs, B., Collin, F., Beazer-Barclay, Y. D., Antonellis, K. J., Scherf, U., and Speed, T. P. (2003). Exploration, normalization, and summaries of high density oligonucleotide array probe level data. Biostatistics *4*, 249–264.

Ishii, M., and Kurachi, Y. (2003). Physiological actions of regulators of G-protein signaling (RGS) proteins. Life Sci. *74*, 163–171.

Karsenty, G., and Wagner, E. F. (2002). Reaching a genetic and molecular understanding of skeletal development. Dev. Cell *2*, 389–406.

Kim, I. S., Otto, F., Zabel, B., and Mundlos, S. (1999). Regulation of chondrocyte differentiation by Cbfa1. Mech. Dev. *80*, 159–170.

Knudson, C. B., and Knudson, W. (2001). Cartilage proteoglycans. Semin. Cell Dev. Biol. *12*, 69–78.

Ko, J. K., Choi, K. H., Kim, I. S., Jung, E. K., and Park, D. H. (2001). Inducible RGS2 is a cross-talk regulator for parathyroid hormone signaling in rat osteoblast-like UMR106 cells. Biochem. Biophys. Res. Commun. *287*, 1025–1033.

Kronenberg, H. M. (2003). Developmental regulation of the growth plate. Nature *423*, 332–336.

Lefebvre, V., and de Crombrugghe, B. (1998). Toward understanding SOX9 function in chondrocyte differentiation. Matrix Biol. *16*, 529–540.

Li, C., and Wong, W. H. (2001). Model-based analysis of oligonucleotide arrays: expression index computation and outlier detection. Proc. Natl. Acad. Sci. USA *98*, 31–36.

Loebel, D. A., Watson, C. M., De Young, R. A., and Tam, P. P. (2003). Lineage choice and differentiation in mouse embryos and embryonic stem cells. Dev. Biol. *264*, 1–14.

Love, B., Rank, D. R., Penn, S. G., Jenkins, D. A., and Thomas, R. S. (2002). A conditional density error model for the statistical analysis of microarray data. Bioinformatics *18*, 1064–1072.

Ma, J., Nishimura, H., Fogo, A., Kon, V., Inagami, T., and Ichikawa, I. (1998). Accelerated fibrosis and collagen deposition develop in the renal interstitium of angiotensin type 2 receptor null mutant mice during ureteral obstruction. Kidney Int. *53*, 937–944.

Marcotte, E. M., Pellegrini, M., Thompson, M. J., Yeates, T. O., and Eisenberg, D. (1999). A combined algorithm for genome-wide prediction of protein function. Nature *402*, 83–86.

Merz, D., Liu, R., Johnson, K., and Terkeltaub, R. (2003). IL-8/CXCL8 and growth-related oncogene alpha/CXCL1 induce chondrocyte hypertrophic differentiation. J. Immunol. *171*, 4406–4415.

Ornitz, D. M. (2001). Regulation of chondrocyte growth and differentiation by fibroblast growth factor receptor 3. Novartis Found. Symp. *232*, 63–76; discussion 76–80, 272–282.

Pacifici, M., Oshima, O., Fisher, L. W., Young, M. F., Shapiro, I. M., and Leboy, P. S. (1990). Changes in osteonectin distribution and levels are associated with mineralization of the chicken tibial growth cartilage. Calcif. Tissue Int. *47*, 51–61.

Reimold, A. M., Grusby, M. J., Kosaras, B., Fries, J. W., Mori, R., Maniwa, S., Clauss, I. M., Collins, T., Sidman, R. L., Glimcher, M. J., and Glimcher, L. H. (1996). Chondrodysplasia and neurological abnormalities in ATF-2-deficient mice. Nature *379*, 262–265.

Reiner, A., Yekutieli, D., and Benjamini, Y. (2003). Identifying differentially expressed genes using false discovery rate controlling procedures. Bioinformatics *19*, 368–375.

Schmid, C. (1995). Insulin-like growth factors. Cell Biol. Int. *19*, 445–457.

Sekiya, I., Vuoristo, J. T., Larson, B. L., and Prockop, D. J. (2002). In vitro cartilage formation by human adult stem cells from bone marrow stroma defines the sequence of cellular and molecular events during chondrogenesis. Proc. Natl. Acad. Sci. USA *99*, 4397–4402.

Shum, L., and Nuckolls, G. (2002). The life cycle of chondrocytes in the developing skeleton. Arthritis Res. *4*, 94–106.

Silvestri, T., Meliconi, R., Pulsatelli, L., Dolzani, P., Zizzi, F., Frizziero, L., Borzi, R. M., and Facchini, A. (2003). Down-modulation of chemokine receptor cartilage expression in inflammatory arthritis. Rheumatology (Oxford) *42*, 14–18.

Stanton, L. A., Sabari, S., Sampaio, A. V., Underhill, T. M., and Beier, F. (2004). p38 MAP kinase signaling is required for hypertrophic chondrocyte differentiation. Biochem. J. *378*, 53–62.

Stricker, S., Fundele, R., Vortkamp, A., and Mundlos, S. (2002). Role of Runx genes in chondrocyte differentiation. Dev. Biol. *245*, 95–108.

Thirunavukkarasu, K., Halladay, D. L., Miles, R. R., Geringer, C. D., and Onyia, J. E. (2002). Analysis of regulator of G-protein signaling-2 (RGS-2) expression and function in osteoblastic cells. J. Cell. Biochem. *85*, 837–850.

Tu, Y., Stolovitzky, G., and Klein, U. (2002). Quantitative noise analysis for gene expression microarray experiments. Proc. Natl. Acad. Sci. USA *99*, 14031–14036.

Tuckermann, J. P., Pittois, K., Partridge, N. C., Merregaert, J., and Angel, P. (2000). Collagenase-3 (MMP-13) and integral membrane protein 2a (Itm2a) are marker genes of chondrogenic/osteoblastic cells in bone formation: sequential temporal, and spatial expression of Itm2a, ALP, MMP-13, and osteocalcin in the mouse. J. Bone Miner. Res. *15*, 1257–1265.

Wang, G., Woods, A., Sabari, S., Pagnotta, L., Stanton, L. A., and Beier, F. (2004). RhoA/ROCK signaling suppresses hypertrophic chondrocyte differentiation. J. Biol. Chem. *279*, 13205–13214.

Watanabe, H., Yamada, Y., and Kimata, K. (1998). Roles of aggrecan, a large chondroitin sulfate proteoglycan, in cartilage structure and function. J. Biochem. (Tokyo) *124*, 687–693.

Watanabe, K., Bruder, S. P., and Caplan, A. I. (1994). Transient expression of type II collagen and tissue mobilization during development of the scleral ossicle, a membranous bone, in the chick embryo. Dev. Dyn. *200*, 212–226.

Weston, A. D., Rosen, V., Chandraratna, R. A., and Underhill, T. M. (2000). Regulation of skeletal progenitor differentiation by the BMP and retinoid signaling pathways. J. Cell Biol. *148*, 679–690.

Weston, A. D., Sampaio, A. V., Ridgeway, A. G., and Underhill, T. M. (2003). Inhibition of p38 MAPK signaling promotes late stages of myogenesis. J. Cell Sci. *116*, 2885–2893.

Zhang, X., Ziran, N., Goater, J. J., Schwarz, E. M., Puzas, J. E., Rosier, R. N., Zuscik, M., Drissi, H., and O'Keefe, R. J. (2004). Primary murine limb bud mesenchymal cells in long-term culture complete chondrocyte differentiation: TGF-beta delays hypertrophy and PGE2 inhibits terminal differentiation. Bone *34*, 809–817.